

Morphological evolution and niche conservatism across a continental radiation of Australian blindsnakes

Sarin Tiatragul (ສາຣິນ ເຕີຍຕະກຸລ) , Alexander Skeels, J. Scott Keogh

Division of Ecology & Evolution, Research School of Biology, The Australian National University, Canberra, ACT, Australia

Corresponding author: Division of Ecology & Evolution, Research School of Biology, The Australian National University, Canberra 2601, ACT, Australia.

Email: sarin.tiatragul@anu.edu.au

Abstract

Understanding how continental radiations are assembled across space and time is a major question in macroevolutionary biology. Here, we use a phylogenomic-scale phylogeny, a comprehensive morphological dataset, and environmental niche models to evaluate the relationship between trait and environment and assess the role of geography and niche conservatism in the continental radiation of Australian blindsnakes. The Australo-Papuan blindsnake genus, *Anilios*, comprises 47 described species of which 46 are endemic to and distributed across various biomes on continental Australia. Although we expected blindsnakes to be morphologically conserved, we found considerable interspecific variation in all morphological traits we measured. Absolute body length is negatively correlated with mean annual temperature, and body shape ratios are negatively correlated with soil compactness. We found that morphologically similar species are likely not a result of ecological convergence. Age-overlap correlation tests revealed niche similarity decreased with the relative age of speciation events. We also found low geographical overlap across the phylogeny, suggesting that speciation is largely allopatric with low rates of secondary range overlap. Our study offers insights into the eco-morphological evolution of blindsnakes and the potential for phylogenetic niche conservatism to influence continental scale radiations.

Keywords: Scolecophidia, niche conservatism, ecological niche model, nonadaptive radiation, reptiles, speciation

Introduction

The coupling of ecological and morphological disparity within an initially rapidly diversifying lineage is the hallmark of adaptive radiation (Czekanski-Moir & Rundell, 2019; Schlüter, 2000). Ecological opportunity is commonly considered the main driver of adaptive radiation because it provides species with geographical, ecological, and evolutionary access to multiple niche axes (Gillespie et al., 2020; Schlüter, 2000; Simpson, 1953; Stroud & Losos, 2016). Among vertebrates, striking examples include *Anolis* lizards of the Caribbean islands (Losos, 2009), Galápagos finches (Grant & Grant, 2014), and cichlids of the African Rift Lakes (Kornfield & Smith, 2000), all of which experienced lineage proliferation from a common ancestor into multiple species with phenotypic adaptations that allow them to occupy divergent ecological niche while co-occurring in sympatry. On the other end of the evolutionary radiation spectrum is nonadaptive radiation, which is defined as the process by which lineages proliferate with minimal ecological niche differentiation (Gittenberger, 1991), and it often (but not always) involves clades with high morphological and ecological niche overlap occurring in allopatry or parapatry (Czekanski-Moir & Rundell, 2019; Rundell & Price, 2009). In these instances, ecological and morphological disparity are decoupled, and eco-evolutionary processes related to phylogenetic niche conservatism, along with geographic isolation, are hypothesized as the main drivers of nonadaptive radiation (Czekanski-Moir & Rundell, 2019; Ramírez-Reyes et al., 2022; Rundell & Price, 2009).

Indeed, a growing body of empirical studies has supported this hypothesis across the animals (Bank et al., 2021; Barley et al., 2013; Bonaccorso et al., 2021; Day et al., 2020; Esparza-Estrada et al., 2023; Gittenberger, 1991; Hausdorf & Xu, 2023; Holland & Hadfield, 2004; Koch et al., 2020; Kozak et al., 2006; Ramírez-Reyes et al., 2022; Reaney et al., 2018; Wake, 2006; Wellenreuther & Sánchez-Guillén, 2016; Wilke et al., 2010; Xu & Shaw, 2020) and plants (Cruz-Nicolás et al., 2021, 2023; Herrando-Moraira et al., 2023). However, most of these studies on animals were done in small areas or islands.

Studies that investigate species-rich clades of terrestrial vertebrates that are morphologically and ecologically conserved on a continental scale are rare (Kozak et al., 2006; Maestri et al., 2017; Reaney et al., 2018). One explanation for this paucity of studies is that the phylogenetic diversity of morphologically and ecologically conserved species is often underestimated (i.e., cryptic species), making them difficult to recognize as evolutionary radiation to begin with (Czekanski-Moir & Rundell, 2019; Demos et al., 2020; Marin et al., 2013b; Olivares et al., 2024; Oliver et al., 2009). How common nonadaptive radiations are on a continental scale and to what spatiotemporal extent niche conservatism can persist in environmentally heterogeneous landscapes remain open questions.

Continental Australia harbors immense biodiversity, most of which is found nowhere else on Earth. Its varied biomes (Byrne et al., 2018), dramatic changes in climate (Byrne et al.,

Received January 23, 2024; revisions received September 5, 2024; accepted September 11, 2024

Associate Editor: Alison Davis Rabosky; Handling Editor: Hélène Morlon

© The Author(s) 2024. Published by Oxford University Press on behalf of The Society for the Study of Evolution (SSE).

This is an Open Access article distributed under the terms of the Creative Commons Attribution-NonCommercial-NoDerivs licence (<https://creativecommons.org/licenses/by-nc-nd/4.0/>), which permits non-commercial reproduction and distribution of the work, in any medium, provided the original work is not altered or transformed in any way, and that the work is properly cited. For commercial re-use, please contact reprints@oup.com for reprints and translation rights for reprints. All other permissions can be obtained through our RightsLink service via the Permissions link on the article page on our site—for further information please contact journals.permissions@oup.com.

2011; Pepper & Keogh, 2021), and past geological proximity to Asia and connection to New Guinea (Oliver & Hugall, 2017) have all stimulated evolutionary radiations that result in the diversity we observed today (Brennan et al., 2023; Cardillo et al., 2017; Couzens & Prideaux, 2018; Crisp et al., 2004; Heterick et al., 2017; Marki et al., 2017; Owen et al., 2017; Roycroft et al., 2022; Skeels et al., 2023). Among Australian terrestrial vertebrates, squamate reptiles (lizards and snakes) represent a species-rich group with over 1,000 species described, many of which have diversified greatly during the Miocene from multiple independent dispersals into the continent (Brennan & Oliver, 2017; Oliver & Hugall, 2017). Some of the most iconic Australian squamate clades show dramatic ecological and morphological diversity including elapid snakes (Grundler & Rabosky, 2014; Lee et al., 2016; Sanders et al., 2008), pythons (Esquerre et al., 2020, 2022), sphenomorphine skinks (Camaiti et al., 2023; Rabosky et al., 2007), agamid lizards (Gray et al., 2019), geckos (Norris et al., 2021), and monitor lizards (Brennan et al., 2021; Pavón-Vázquez et al., 2022). However, a few other clades have also undergone extensive lineage diversification, but with more subtle ecological and/or morphological divergence, such as subsets of *Heteronotia* geckos (Moritz et al., 2016; Zozaya et al., 2019), eugongyline lizards (Schneider & Moritz, 1999; Singhal et al., 2018), *Ctenotus* skinks (Prates et al., 2023), earless dragons (Chaplin et al., 2020), and blindsnares (Marin et al., 2013b; Shine & Webb, 1990).

Snakes in the subfamily Scolecophidia, commonly known in English as “blindsnares” or “threadsnakes,” have a highly specialized phenotype that makes them well-suited for strict fossoriality (Da Silva et al., 2018), yet surprisingly little is known about their ecology, morphology, and evolutionary history (Miralles et al., 2018). There are ~450 species described species of scolecophidians in five families (Uetz et al., 2021), four of which form a monophyletic clade that split off early in the evolution of all extant snakes, and one family (Anomalepididae) is sister to all modern Alethinophidia snakes, rendering Scolecophidia paraphyletic (Burbrink et al., 2020; Miralles et al., 2018). The Australo-Papuan blindsnares genus *Anilios*, in the family Typhlopidae, is the most speciose among Scolecophidia, making them an ideal model system to test hypotheses about drivers of speciation in an ecologically specialized group on an ecologically diverse continent. Previous studies have shown that Australian blindsnares radiated rapidly in the early Miocene from mesic-adapted ancestors of Asian or Melanesian origin (Marin et al., 2013a; Tiatragul et al., 2023b; Vidal et al., 2010). Of the 47 formally described species of *Anilios* (Tiatragul et al., 2023a), 46 are distributed across Australia, apart from the New Guinean endemic, *A. erycinus*. Species occur in all the major biomes on the continent, from the arid interior to the mesic continental margins (Tiatragul et al., 2023b). Despite the diversity and distribution of blindsnares throughout Australia, little is known of their natural history because their fossorial lifestyle makes them challenging to observe in situ (Ehmann & Bamford, 1993). Examinations of preserved museum specimens revealed that at least 10 species of Australian blindsnares primarily feed on broods of pupae and larvae of ants and termites (Webb & Shine, 1993a). Follow-up studies found interspecific variation in size and the presence of sexual size dimorphism in several species where females are larger than males (Shine & Webb, 1990; Webb & Shine, 1993b). To date, no study has extensively quantified the extent of

morphological variation in the group and its association with ecological factors that may have influenced speciation of this continental radiation.

In this study, we generated the most comprehensive eco-morphological dataset to date for *Anilios* blindsnares and applied a suite of phylogenetic comparative methods to investigate the relationship between morphological and ecological traits to understand the ecological context of this continental radiation. We further tested for a signal of niche conservatism and estimated the dominant mode of speciation using a combination of phylogenetic comparative methods and ecological niche models (ENMs). Specifically, we ask: (1) What are the main axes of morphological variation? (2) Does variation in morphology among species correlate with their current environments? (3) Are lineages that occupy ecologically similar habitats morphologically convergent? (4) Is speciation predominantly allopatric or sympatric? (5) Do sister species have greater morphological and ecological niche overlap than expected relative to nonsister species pairs? We predict that if species have diverged in sympatry, closely related species should exhibit significant morphological variation that corresponds to divergent ecological niches. If species are speciating mostly via allopatric speciation, we would expect closely related species to show some variation in morphology but a significantly high level of niche conservatism and a low level of geographic overlap.

Materials and methods

Specimen sampling

We examined 496 specimens representing all 47 formally described species of *Anilios* (Uetz et al., 2021) along with closely related representatives of Australo-Papuan blindsnares in the family Typhlopidae, including *Acutotyphlops subocularis*, *Ramphotyphlops acuticauda*, *R. depressus*, and *R. multilineatus* (Supplementary Table S1). Our sample size per species ranged from 1 to 26 specimens (median = 8 specimens). We measured the specimens from the South Australian Museum (SAMA), Western Australian Museum, Queensland Museum, Museum and Art Gallery of the Northern Territory (MAGNT), Australian National Wildlife Collection, Florida Museum of Natural History (FLMNH), and the Natural History Museum Berlin (ZMB), and a private collection. Where possible, we selected relatively large male and female specimens with well-preserved heads to quantify variation in snout shape. The sex of specimens was determined by the presence of everted hemipenes or dissecting the specimen to inspect the gonads (73%); if neither was possible, sex was assigned based on relative tail lengths measured in this study (17%), otherwise left as unknown (10%). We included data from the literature for *A. erycinus* (Werner, 1901) and *A. batillus* (Waite, 1894) as we were unable to access the specimens in person.

Phylogeny and taxon sampling

For all phylogenetically informed analyses, we used the subset of the time-calibrated phylogeny of Australian blindsnares with outgroups from (Tiatragul et al., 2023a). This phylogeny was inferred using the shortcut coalescent method in ASTRAL III (Zhang et al., 2018) based on 4,930 maximum likelihood gene trees estimated using IQTREE (Minh et al., 2020). Divergence dating was carried out using MCMCTree from the PAML package (Yang, 2007) using 27 outgroup

squamate reptile fossil calibrations (Tiatragul et al., 2023a). The phylogeny includes 37 taxa representing 35/47 formally described species of *Anilios*. Two additional genetically distinct lineages, the eastern population of “*A. grypus*” and the eastern population of “*A. ligatus*,” were also included based on their genetic divergence and geographical distinction (Tiatragul et al., 2023a). We also present data for the rest of *Anilios* species along with closely related outgroups in which there is no phylogenetic data.

Morphological data

Body size, body shape, tail-length, and head shape are important traits that influence locomotion and food acquisition in limbless terrestrial burrowing animals (Gans, 1960, 1975). We assembled morphological datasets comprising linear morphometrics measurements of the body and landmark-based geometric morphometrics assessment of the dorsal surface of the head ($n = 489$). For body size and linear morphometrics datasets, we measured snout-to-vent length (SVL) as a proxy for body size, tail-length, and four external characters that describe body shape variation: midbody diameter (MBD), midtail width (MTW), head width (HWE), and head depth (Supplementary Figure S1). We measured SVL and tail-length by carefully stretching the specimen along a ruler to the nearest 0.5mm. The rest of the measurements were measured using a digital vernier caliper (ABS Coolant Proof Caliper, Mitutoyo, Japan) to the nearest 0.1 mm. To obtain mean shape ratios (Mosimann, 1970) for each species, we divided each linear measurement by SVL. These sets of shape ratios were then log-transformed for further analyses (henceforth referred to as body shape ratios).

Variations in the head shape of blindsnakes, particularly the snout, have been hypothesized as adaptation to different soil characteristics (Ehmann & Bamford, 1993). For each specimen examined, we photographed the dorsal surface of the head with a Canon 80D camera fitted with an EF 100mm F/2.8 macro USM lens (Canon Inc, Tokyo, Japan) and illuminated with Yongnuo YN-24EX TTL macro flash (Yongnuo, Shenzhen, China) mounted on a tripod above the specimen. We placed a ruler next to each specimen in the photograph as a scale bar. Based on these head photographs and images from the literature ($n = 3$), we used tpsDig 2.17 (Rohlf, 2015) software to digitize 10 fixed landmarks and four sets of curves each with five or three equidistant semilandmarks that are allowed to slide with minimize bending energy (Gunz & Mitteroecker, 2013) between fixed points to represent the features and curvature of the snout from the dorsal view (Supplementary Figure S2). We superimposed landmark coordinates for each specimen by Generalized Procrustes Analysis using “gpaen” function in the R package geomorph v.4.0.6 (Adams et al., 2022; Baken et al., 2021) to remove the effects of scale and orientation and calculate centroid size of the head, which is the square root of the sum of the squared distance of landmarks to the center of the landmark configuration. We further accounted for object symmetry using the function “bilat.symmetry” and extracted the symmetric component for further analyses. We also accounted for sexual size dimorphism in both body shape ratios and snout shape datasets (Supplementary Methods; Supplementary Tables S2–S10).

Morphological variation

To examine the variation in body shape ratios and snout shape among the species, we performed conventional principal

component analyses (PCA) on the full dataset and phylogenetic PCAs (phy-PCA) on a subset of species that are in the phylogeny. We used the “prcomp” function in R to perform the conventional PCA. Since phylogenetic PCA are prone to biases associated with misidentification of evolutionary models (Uyeda et al., 2015), we first fitted four different evolutionary models to multivariate traits dataset—Brownian motion (BM), Ornstein-Uhlenbeck (OU), Early Burst (EB), and Pagel’s λ (lambda)—using “mvgl” in mvMORPH v.1.1.6 (Clavel et al., 2015, 2019). We assessed the relative fit of these evolutionary models for each multivariate dataset with the Akaike Information Criterion and Generalized Information Criterion and used output covariance matrices from the best-fitting models to estimate the phy-PCAs (Supplementary Methods). We accounted for static allometry in the snout shape dataset by adding log centroid size as a covariate and used the regression residuals to represent size-free variation of snout shape in the PCA (Klingenberg, 2016). To visualize how body and snout shapes vary across the phylogeny, we projected the first two PC axes along with the phylogeny onto their morphospaces using the “phylomorphospace” function from the R package phytools v.1.2 (Revell, 2012). We generated thin-plate deformation plots that compared the PC extremes to a reference global mean using the function “plotRefToTarget” from geomorph to aid visualization.

Occurrence data

Occurrence data were based on locality records of preserved specimens from museum databases and verified human observations from Atlas of the Living Australia (ALA). We modified some records to reflect the latest taxonomic changes based on the updated distribution range and ST’s examination of specimens. We discarded records with identical latitude and longitude, as well as records with uncertain taxonomic identities. In total, we retained 3,898 verified records (per species min = 1, median = 23, mean = 81, max = 525) representing every species of Australian *Anilios* for our analyses (See data availability statement).

Environmental data

We selected soil bulk density, annual mean temperature, and aridity index as the most biologically interpretable variables to describe blindsnake niches. Soil bulk density measures the penetrability of soil, which is relevant for strictly fossorial reptiles (Camaiti et al., 2023). Mean annual temperature serves as a climate proxy, a commonly used technique to describe niches for squamate reptiles (Cox & Cox, 2015; Pie et al., 2017; Wiens et al., 2013). Finally, the aridity index reflects precipitation availability over atmospheric water demand and is categorized as follows: hyper arid, < 0.03 ; arid, 0.03–0.2; semiarid, 0.2–0.5; dry subhumid, 0.5–0.65; humid, > 0.65 (Zomer et al., 2022). From raster files that contained modeled approximations at the resolution of 3 arc-seconds, we extracted soil bulk density values between 0 and 5 cm depth from CSIRO Soil and Landscape Grid of Australia, mean annual temperature from WorldClim v.2 (Fick & Hijmans, 2017), and aridity index from Zomer et al., (2022) for each georeferenced record using the “extract” function in the R package raster v.3.6–3 (Hijmans, 2023). We then calculated the maximum soil bulk density, mean annual temperature, and mean aridity index for each species. Correlation analyses revealed that none of the background environmental variables were strongly correlated (Pearson’s $r < |0.75|$).

To test whether ecologically similar species converge in morphology, we first assigned species as humid or arid based on aridity index values to reflect ecological extremes (arid < 0.2; humid > 0.65). We further subdivided arid species into different types of desert landscapes (Mabbutt, 1988) based on their distribution and habitat description from the primary literature. In summary, we tested for convergence among four humid species, eight dune desert species, eight upland desert species, six stony desert species, and eight shield plains species. Nine species are assigned to more than one desert type due to their range (Supplementary Methods).

MaxEnt ecological niche models

To get realistic estimates of the species distributions and calculate overlaps in geographic and ecological niche, we first built ENMs for each species that had ≥ 5 occurrence records ($n = 32$ species) by fitting occurrence records and the three environmental predictors using the presence-only algorithm of Maximum Entropy (MaxEnt) v.3.4.4 (Elith et al., 2011) implemented with “enmtool.maxent” in the R package ENMTools v.1.1.1 (Warren et al., 2021). We accounted for spatial sampling bias by creating a kernel density map estimated from all *Anilius* occurrence data using the function “biaslayer” in the R package ntbox (Osorio-Olvera et al., 2020). For each ENM, we withheld 20% of occurrence data randomly for model evaluation, specified 1,000 background points to be sampled, and 10,000 points to be drawn from environment space for environment space discrimination metrics. We used default values for all other MaxEnt parameters. To confirm our results are consistent even when six ENMs were built on a low number of occurrence records ($n < 20$), we repeated all analyses that rely on ENMs with a subset of taxa ($n = 26$ species) that has ≥ 20 occurrence records. We evaluated ENMs by the Area Under the receiver operating characteristic Curve (AUC). Additionally, we computed variable importance scores for each ENM using the “vi_permute” function in the R package vip (Greenwell & Boehmke, 2020).

Statistical analyses

Environmental correlates with morphology

To test if variation in morphology among species strongly correlates with their current environment, we fitted separate phylogenetic linear regressions for each trait dataset and evaluated model fit to determine which ecological predictors best-explained variation in morphological traits. We used a maximum likelihood approach to fit univariate regressions for body size (log maximum SVL) using the R package phylolm (Ho & Ane, 2014) and multivariate regressions for body shape ratios using Generalized Least Squares implemented in the “mvgl” function of mvMORPH. We used a penalized likelihood approach to fit linear models to our high-dimensional landmark-based snout shape dataset (Clavel et al., 2019). In all models, we specified Pagel’s λ as the error term as this corresponds to fitting a phylogenetic mixed model, which accounts for deviations from BM and offers greater flexibility in estimating the error structure while jointly estimating the phylogenetic signal (Clavel & Morlon, 2020).

We first fitted each morphological dataset against all environmental predictors together and assessed the significance of each predictor with Type III (sums of squares) phylogenetic MANOVAs using both parametric and permutation tests (Supplementary Methods). We then removed nonsignificant

predictors iteratively until all remaining variables were statistically significant. We evaluated model fit with either the Akaike Information Criterion for the maximum likelihood models or with the Extended Information Criterion for the penalized likelihood model.

Convergence measures

We used two main approaches to quantify if *Anilius* species that occupy ecologically similar habitats independently show convergence in body shape and snout shape (PC1 and PC2). First, we calculated the distant-based C_t -measures (Grossnickle et al., 2024) and the frequency-based C_5 measure of convergence using functions in the R package convevol v.2.0.1 (Stayton, 2015). Positive C_t values indicate different degrees of convergence up to 1 (complete convergence), while 0 and negative values indicate a lack of convergence (Grossnickle et al., 2024). We grouped closely related species in the same habitat to avoid uninformative comparisons (Supplementary Methods). We calculated C_5 , which measures the number of lineages that cross into the morphospace region of interest from outside; we used PC1 and PC2 of body shape ratios instead of the five-trait multivariate data set. We tested for statistical significance by comparing the observed C_t -measures with a null distribution of simulated evolution ($n = 500$) according to BM (Supplementary Methods). Second, we used a model-fitting approach to determine if evolutionary models where lineages are evolving toward distinctive trait optima or adaptive peaks provide a better fit than other models of evolution. Using mvMORPH, we first fitted a single-rate multivariate BM model (mvBM1), a single optimum OU model (mvOU1), and an early burst model (mvEB) to the trait data. We then fit a multivariate OU model with two selective regimes (mvOU2) where arid and humid species are allowed to have different trait optima and the multirate and multiselective regime BM model (mvBMM) as another null model. To determine the best-fit model, we compared the relative Akaike weights (AICw) for each model. Phylogenetic comparative methods may have low power to detect processes when sample size is low. To determine whether the *Anilius* phylogeny (37 species) used in this study is sufficient to detect possible convergent evolution, we performed a power analysis using simulations (details in Supplementary Methods and Results). We show that our phylogeny has enough power to detect convergence using the model selection approach, even when the difference between trait optima is small (Supplementary Appendix Tables R1–4). We found that using C_t -measures, significant levels of convergence could be detected when trait optima were very different, but this power decreased as trait optima became more similar (Supplementary Appendix Figure R2). Taken together, our observed results showing the absence of convergence are likely true negatives.

Age-overlap correlation

The intercept and slope of the relationship between the relative age of divergences and the degree of overlap of diverged species in various traits can help us infer the dominant mode of speciation and how the level of overlap evolved over time (Barracough & Vogler, 2000). We used the “enmtools.aoc” function from ENMTools to conduct age-overlap correlation (AOC) tests to examine how overlaps in ecological niches and morphological traits changed over time in the context of the given phylogeny. Pairwise geographical range overlaps were

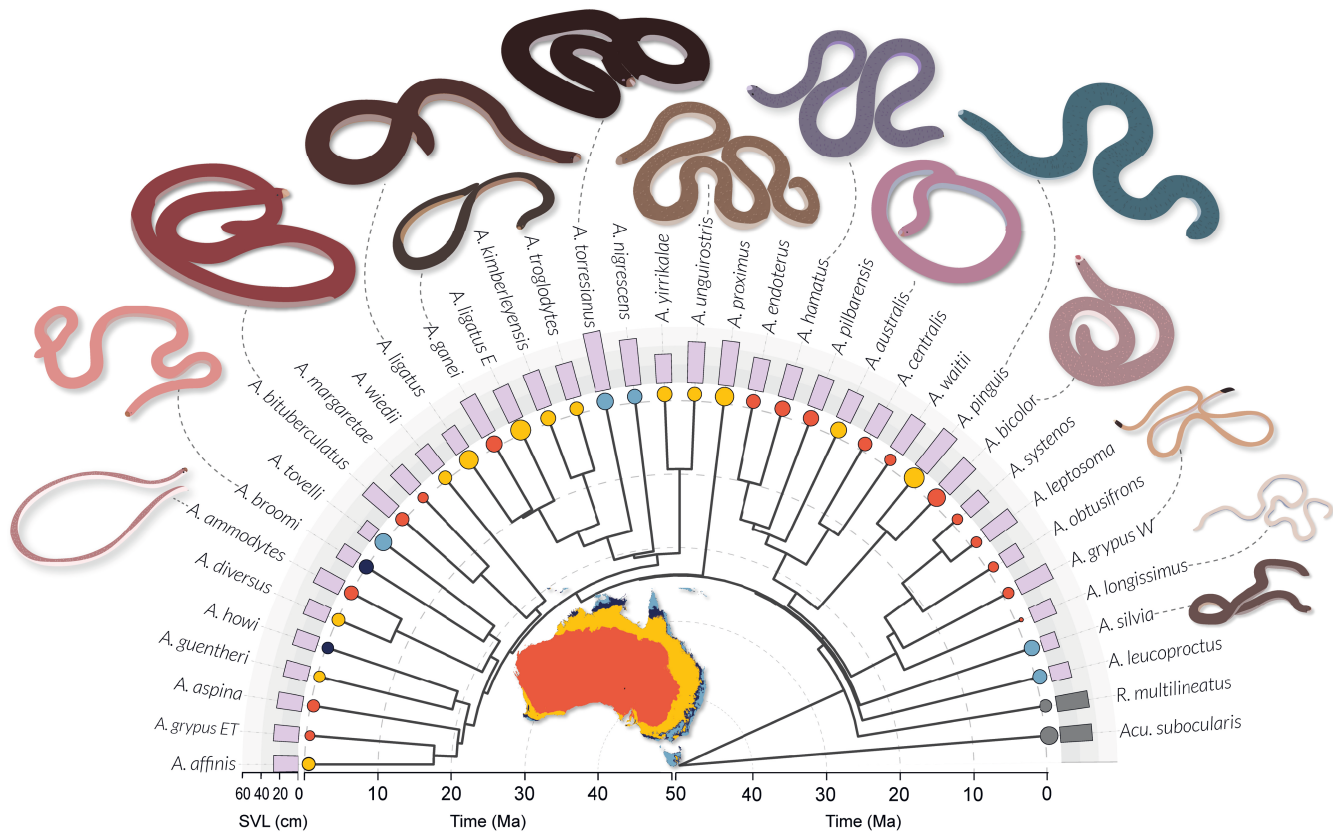


Figure 1. Variation in maximum length and relative MBD/SVL ratio across the phylogeny for Australo-Papuan blindsnakes and close relatives. Bars indicate the absolute maximum snout-vent length. The dot size at the tips represents the ratio of MBD/SVL relative to the mean. The inset map of Australia shows the aridity index, and the colors of the dots at the tips for each species correspond to the aridity index based on species distribution. Blindsight illustrations show approximate variations of body size and shape across the phylogeny. Illustrations were based on photographs from B Bush, R Browne-Cooper, S Eipper, B Schembri, B von Takach, and SM Zozaya.

calculated by dividing the area of overlap between two species ranges by the smaller two area of the species' individual ranges (Fitzpatrick & Turelli, 2006). The value for niche overlap is based on the similarity metric derived from Hellinger's I , calculated using "env.overlap" function in ENMTools. To assess morphological overlap between species, we calculated species pairwise differences in the mean of log(MBD/SVL) as the univariate proxy for body shape and mean snout shape calculated from "mshape" function in geomorph (Supplementary Methods). We conducted AOC tests for geographical range ($n = 32$ species), ecological niche ($n = 32$ species), log relative body width to body size ($n = 37$ species), and snout shape ($n = 37$ species). We determined statistical significance by comparing the empirical intercept and slope to those generated from 100 Monte Carlo replicates, each time randomizing the identity of the tips of the tree and repeating the node averaging and modeling steps.

Comparing overlaps between sister species and nonsister species pairs

AOC analyses may give inconclusive results when speciation involves a mixture of allopatric or sympatric speciation rather than a single dominant speciation mode or when postspeciation range shifts obscure the geographic information about speciation (Fitzpatrick & Turelli, 2006). As such, we also test whether sister species have greater overlap in each metric than their next closest relatives using pairwise distance analysis (Freer et al., 2022). We identified 11 species pairs and

chose the most recently diverged species from each sister species pair as the nonsister species. For each overlap metric, we calculated the difference between sister pairs and the averaged distance between each of the sister species to their nonsister species. Our phylogeny is incompletely sampled, which means we may not have all true sister species pairs present. Nevertheless, the expectation remains the same regardless of the phylogenetic resolution—closely related taxa should have more (or less) overlap than more distantly related taxa. As such, overlap tests and AOC are useful tools to assess patterns that may be indicative of historical speciation mode. We then use the "binom.test" function in the stats package to conduct an exact binomial test to assess whether the observed frequency (f) of sister pairs that have greater overlaps compared to their averaged nonsister pairs were greater than expected by chance.

Simulation-based speciation mode inference

To investigate the relative support for the prevalence of different geographic modes of speciation throughout the radiation of blindsnakes, we used a simulation-based inference approach based on the Dynamic Range Evolution and Diversification simulation model (DREaD) (Skeels & Cardillo, 2019). DREaD models uncertainty about the degree of range shifting and extinction throughout the history of different clades by including parameters that drive geographic range dynamics, including dispersal, environmental niche evolution, and environmental change. We estimated 14

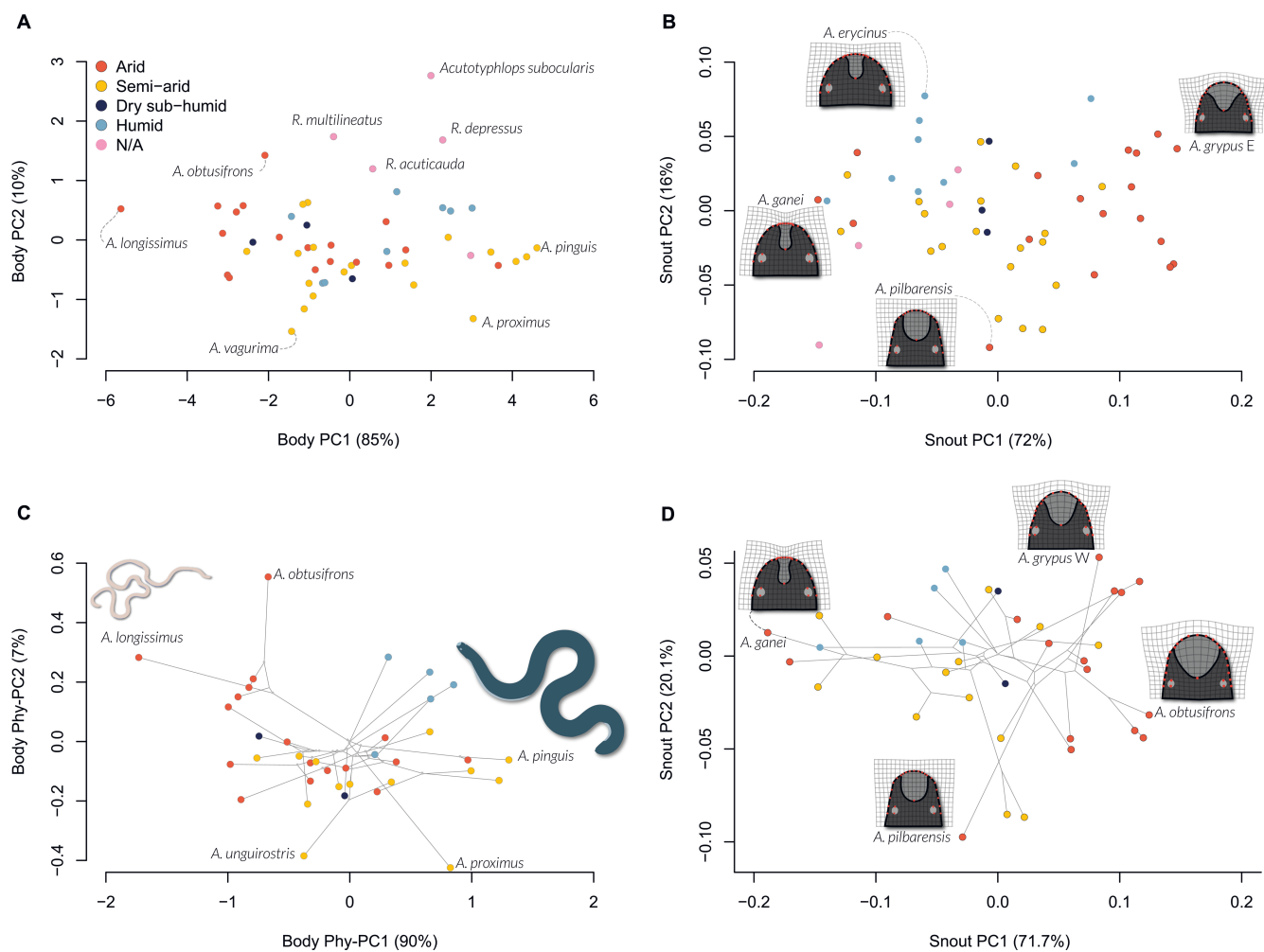


Figure 2. Variation in body shape ratios and snout shape of Australo-Papuan blindsnakes and close relatives. Values are from Principal Component Analyses (PCA) and Phylogenetic PCA (phy-PCA). (A) PCA plot of body shape ratios. (B) PCA plot of snout shape based on landmark-based geometric morphometrics. (C) Phy-PCA of body shape ratios. (D) Phy-PCA of snout shape. For (B) and (D), thin-plate deformation plots represent species that represent the extremes and unusual phenotypes compared to the global mean snout shape. Dot colors represent the category of habitat ranging from arid to humid based on species occurrence.

summary statistics used to infer the geography of speciation with DREaD from phylogenetic and geographic data. We estimated species geographic ranges using two alternative approaches based on the filtered occurrence records. First, we extended a circular buffer around each occurrence point, and to account for uncertainty in this approach, we used two buffer sizes—30 km and 50 km. Second, we estimated the minimum convex polygon of the species occurrence records that includes at least 90% of the records. We then used two Approximate Bayesian Computation algorithms (neural net and multinomial logistic regression) to estimate the posterior probabilities of each speciation mode with the R package abc (Csilléry et al., 2012). We trained the models using the simulated dataset from Skeels and Cardillo (2019).

Results

Main axes of morphological variation among *Anilius* blindsnakes

For body shape, the main axis of variation is how wide the snake is relative to its length (body PC1 = 85%; body Phy-PC1 = 89%), while size-corrected tail-length explained

most of the variation in the second axis of variation (body PC2 = 10%; body Phy-PC2 = 7%). The most extreme phenotypes of PC1 and phy-PC1 are represented by the slender and narrow *A. longissimus* on one end and the plump and wide *A. pinguis* on the other end (Figure 1; Figure 2A–C). *Anilius* species at the extremes of PC2 are *A. obtusifrons* and *A. vagurima* (Figure 2A), while the extremes of phy-PC2 are represented by *A. obtusifrons* and *A. unguirostris* (Figure 2C). Outgroup species including *Ramphotyphlops* and *Acotyphlops* clustered with higher body shape PC2 values than all *Anilius* species except *A. obtusifrons*. Of all the *Anilius* specimens measured, we found that the species with the longest absolute maximum SVL is *A. torresianus* at 640 mm, and the shortest is *A. silvia* at 71 mm (Figure 1).

Variation in dorsal snout shape is mostly explained by rostrum width (snout PC1 = 72%; snout Phy-PC1 = 69%), with *A. tovelli* and the western lineage of *A. grypus* representing the narrowest and widest configuration of landmarks for the rostral scale, respectively (Figure 2B and D; Supplementary Figure S3). The second axis of variation for dorsal snout shape is characterized by variation in relative distance between eyes to the tip of the snout (snout PC2 = 16%; snout

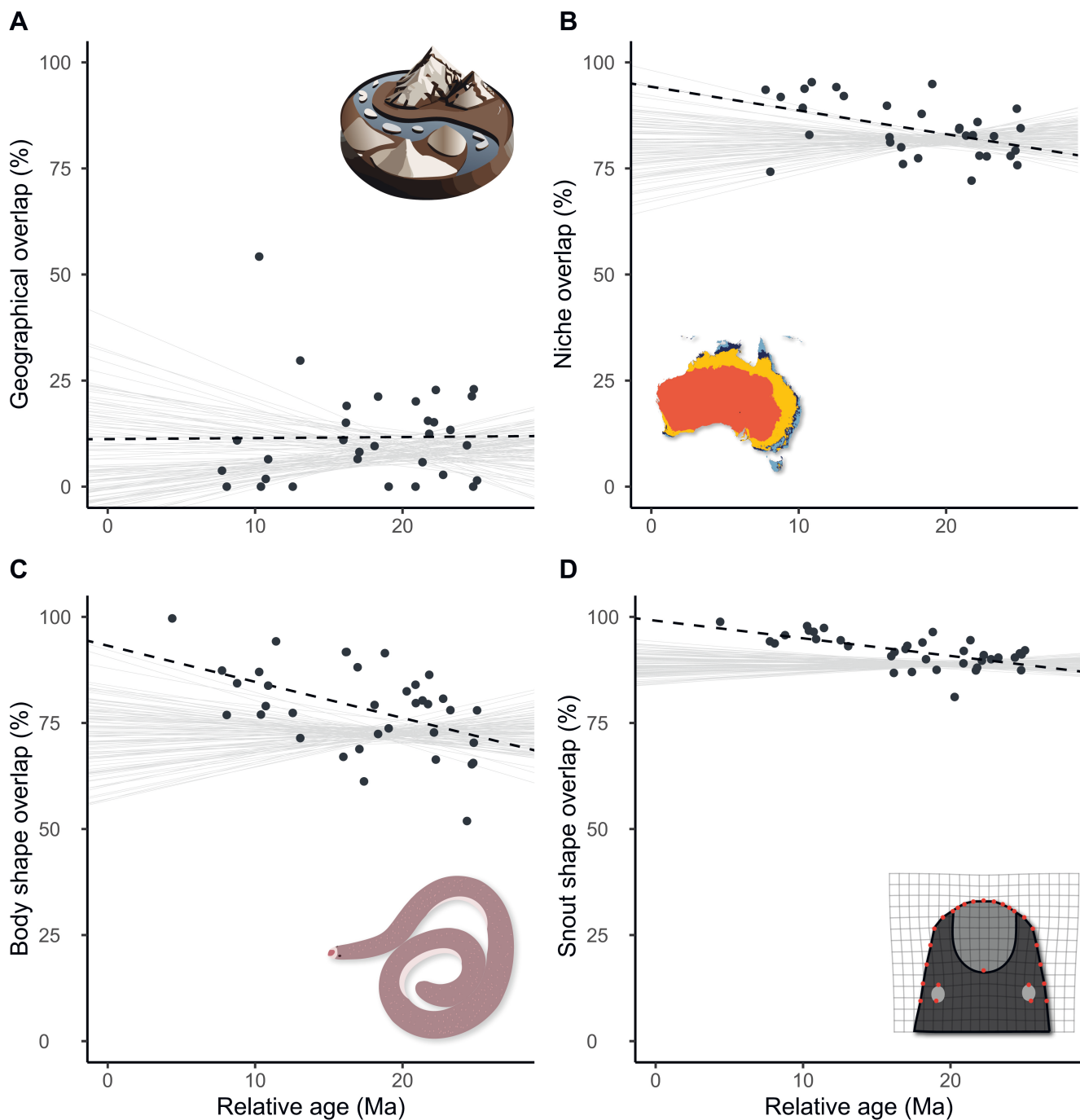


Figure 3. Relationship between relative age of species divergence and overlaps in (A) geographic range, (B) ecological niche, (C) body shape (log of MBD/SVL), and (D) snout shape. Points represent the value in the overlap metrics and the relative age of the nodes in the phylogeny. Solid lines represent the slopes from 100 Monte Carlo iterations, and dashed lines represent the slope from the empirical age-overlap correlation regression. Empirical intercepts and slopes are significantly different than the null model iterations for (B), (C), and (D). These results suggest that recently diverged species have greater ecological niche overlap, body shape overlap, and snout shape overlap than distantly related species.

phy-PC2 = 20%). Extremes for snout PC2 are represented by *A. erycinus* (“rounder snout”) and *A. pilbarensis* (“narrower snout”), while extremes for snout phy-PC2 are represented by *A. leucoproctus* and *A. pilbarensis* (Figure 2B and D). Closely related species tend to cluster in morphospace for both body shape ratios and dorsal snout shape (Figure 2C and D).

Environmental predictors of morphological variation

We used a combination of univariate and multivariate phylogenetic linear regressions to assess whether variation in

morphology among species correlates with their current environment. Prior to fitting the phylogenetic linear regressions, we assessed the performance of different models of trait evolution. The best-fitting trait evolution models based on maximum likelihood was the EB model for the univariate log maximum SVL ($Z = 5.68$, $\sigma^2 = 0.07$, $b = -0.63$, AIC_w = 0.66; Supplementary Table S11), and jointly Pagel’s λ (AIC = -199.24) and BM (AIC = -199.24) for multivariate body shape ratio (Supplementary Table S12). The best-fitting trait evolution model for snout shape based on penalized likelihood was also jointly Pagel’s λ and BM (GIC = -33891;

Supplementary Table S13). Variance–covariance matrices for these models were used to calculate phy-PCAs. We found a moderate phylogenetic signal for log maximum SVL (phyloM $\lambda = 0.85$) and snout shape (mvMORPH $\lambda = 0.77$) and a strong phylogenetic signal for body shape ratios (mvMORPH $\lambda = 0.98$).

Our best-fitting univariate phylogenetic linear regression, where temperature is the only predictor in the model ($AIC_w = 0.37$; **Supplementary Table S14**), revealed a negative correlation between log maximum body size and temperature ($\beta = -0.03 \pm 0.01$ SE, $\lambda = 0.79$, $\sigma^2 = 0.003$, $p = 0.037$). Neither variation in soil bulk density nor aridity index had a significant influence on the variation in maximum body size ($p > 0.05$; **Supplementary Table S14**). These results indicate that, in general, species that are larger in SVL inhabit cooler areas, while shorter species inhabit warmer areas. We also found that the averaged species aridity index and soil bulk density values were highly correlated (Pearson's $r = -0.84$), which might partially explain why the simpler model was preferred over the full model.

From the mvMORPH multivariate analyses of body shape ratios, while we found that both aridity index and soil bulk density have statistically significant effects, we only report the result from our best-fitting model where soil bulk density is the only predictor ($AIC_w = 0.99$; **Supplementary Table S15** for coefficients from all models). We found that body shape ratios negatively correlated with soil bulk density ($\lambda = 1$, $df = 1$, $F = 2.94$, $p = 0.037$). Temperature had no statistically significant influence on variation in body shape ratios (**Supplementary Table S15**). These results indicate that body shape varies in a correlated way with both soil bulk density and aridity index. However, because the two predictors are correlated, the model cannot distinguish their respective importance. Our data suggest that species that have more “robust” body shape ratios tend to occupy soil with lower bulk density and inhabit more humid areas, while species that have more “skinny” body shape tend to occupy soil with higher bulk density and more arid areas. Finally, we found no correlation between landmark-based dorsal snout shape and any environmental predictors (**Supplementary Table S16**).

Morphological convergence

We used multiple approaches to test whether species that occupy ecologically similar habitats have independently converged in morphospace (**Supplementary Figure S4**). Distance-based $Ct1$ scores for body shape ratios were negative for species in all types of habitats: humid species ($Ct1 = -6.4$, $p = 0.108$), dune desert species ($Ct1 = -0.48$, $p = 0.152$), upland desert species ($Ct1 = -0.27$, $p = 0.05$), stony desert species ($Ct1 = -0.64$, $p = 0.21$), and shield plains species ($Ct1 = -0.36$, $p = 0.10$). Although not statistically significant, negative scores indicate a lack of support for convergence in body shape ratios (**Supplementary Table S17**). Similarly, we found negative $Ct1$ scores for snout shape indicating no support for convergence in all types of habitat: humid species ($Ct1 = -2.5$, $p = 0.002$), dune desert species ($Ct1 = -0.75$, $p = 0.50$), upland desert species ($Ct1 = -0.68$, $p = 0.49$), stony desert species ($Ct1 = -0.56$, $p = 0.20$), and shield plains species ($Ct1 = -0.41$, $p = 0.15$; **Supplementary Table S18**). Frequency-based $C5$ scores for PCs of body shape ratios and snout shape indicate that the number of lineages converging to a unique region of morphospace is small and not significant for any arid desert groups ($p > 0.05$; **Supplementary**

Table S17–S18). However, within humid species, all four lineages enter a particular region of morphospace for PCs of body shape ratios and snout shape, a statistically significant result for body shape ratio ($p = 0.044$) but not for snout shape ($p = 0.128$). From the model-fitting approach, we found the best-fitting evolution model based on maximum likelihood for body shape ratios was the multivariate BM model (mvBM1, $AIC_w = 0.79$) followed by the multivariate early burst (mvEB, $AIC_w = 0.21$). All models except the mvBMM were preferred over the mvOU2 model (**Supplementary Table S19**). For snout shape, the best-fitting model was the mvEB model ($AIC_w = 0.74$) followed by mvBM1 ($AIC_w = 0.25$). All other models were preferred over the mvOU2 model for snout shape (**Supplementary Table S20**). These results indicate poor support for models where lineages are evolving traits towards distinct optima, suggesting no convergence evolution.

Dominant mode of geographic speciation

We used range-overlap correlation tests (AOC with geographic range) and simulation-based DREaD models to determine the predominant mode of speciation. From the AOC test between geographic range and relative age, we found a pattern that is consistent with the predictions of allopatric speciation ([Fitzpatrick & Turelli, 2006](#)), where geographical overlap in more closely related species is low ($y = 0.11$, $p = 0.39$) and higher in more distantly related species ($\beta = 0.0003$, $p = 0.49$; **Figure 3A**), but differences are not significant. An analysis using a subset of taxa with well-represented occurrence data found a similar pattern (**Supplementary Results**). Using DREaD to estimate the predominant mode of speciation with three alternative geographic range estimation methods and two alternative ABC algorithms, we found the strongest support for an allopatric-dispersal model of speciation and moderate support for a parapatric model (**Supplementary Figure S5**). Larger buffer distances (30 km and 50 km) led to greater support for an allopatric-dispersal mode in all cases, and a mixed model of speciation also had similar support in the 30 km buffer using the neural network algorithm (mixed = 0.37, allopatric-dispersal = 0.45). The smallest buffer distance (10 km) led to more equal support between allopatric-dispersal ($mnL = 0.38$, $NN = 0.427$) and parapatric ($mnL = 0.38$, $NN = 0.36$) and the minimum convex hull approach both led to greater support for parapatric speciation (NN) and mixed modes (mnL). Both allopatric-dispersal and parapatric models of speciation are characterized by highly asymmetric range sizes during speciation. We found low support for allopatric-vicariance, which is characterized by more symmetrical range sizes, or sympatry, which is characterized by high geographic range overlap.

Phylogenetic niche and morphological conservatism

Overlaps in environmental niches across the phylogeny offer clues about the presence of phylogenetic niche conservatism. Only 1/35 ENMs built had $AUC_{test} > 0.7$ (*A. margaretae* $AUC_{test} = 0.54$), which indicates our ENMs have good discrimination between presence and absence (**Supplementary Table S21**). Based on 100 Monte Carlo permutations of the ENMs, we found that annual mean temperature had the highest averaged importance at $55.11 \pm 23.86\%$, followed by aridity at $40.30 \pm 5.58\%$ and soil bulk density at $4.56 \pm 5.58\%$ (**Supplementary Table S21**).

From analyzing the relationship between ecological niche overlap and relative age, both observed intercept and slope

values were significantly different than expected from null model iterations ($y = 0.94, p = 0.039; \beta = -0.0056, p = 0.049$; Figure 3B). This result, although marginally significant, indicates that more closely related species have greater ecological niche overlap than expected by chance and that niche overlap decreases as relative node age increases, a pattern consistent with niche conservatism. Similarly to the range-overlap correlation test, we repeated this analysis with a subset of taxa and found a similar result (Supplementary Results).

Empirical intercepts and slopes between both morphological traits and relative age were greater than expected from the null model iterations, consistent with the results from phylogenetic signal analyses. More recently diverged species tend to have more similar body shape ratios than distantly diverged species ($y = 0.93, p = 0.0099; \beta = -0.0085, p = 0.030$; Figure 3C). A similar trend is observed between overlap in mean snout shape and relative age ($y = 0.99, p = 0.0099; \beta = -0.0042, p = 0.0099$; Figure 3D). These results indicate phylogenetic morphological conservatism.

Comparison between sister species and nonsister species pairs

We compared 11 sister species with 11 nonsister species pairs that have ENMs and found that the proportion of sister species pairs that had greater overlap in geographic range and ecological niche was not greater than expected by chance. Geographic range overlap is low for both sister pairs ($12\% \pm 17\%$) and nonsister pairs ($10\% \pm 16\%, f = 55\%, p = 1$), indicating low levels of co-occurrence between sister species across the phylogeny (Supplementary Figure S6). Ecological niche overlap was higher in sister pairs ($I = 90 \pm 8\%$) than nonsister pairs ($I = 83 \pm 6\%$), but these differences were not greater than expected by chance ($f = 73\%, P = 0.23$). Exact binomial tests using a subset of taxa with well-represented occurrence data yielded consistent results (Supplementary Results).

From comparing 11 sister species pairs and their corresponding nonsister species, we found significantly greater overlap in snout shape between sister species (overlap = $95 \pm 3\%$) compared to nonsister species (overlap = $90 \pm 4\%, f = 92\%, p = 0.006$). Overlap in body shape is high for both sister pairs ($82 \pm 9\%$) and nonsister pairs ($82 \pm 10\%$) but not significantly different ($f = 33\%, p = 0.39$).

Discussion

Australian blindsnakes offer a good system to test hypotheses about the roles and prevalence of niche conservatism in continental radiation of an ecologically and morphologically conserved group. Here, we used a diverse set of approaches to analyze a comprehensive eco-morphological dataset of Australian blindsnakes to investigate the ecological context of continental radiation. We first discuss the correlation between morphology and environment, then turn to the absence of ecological convergence, and finally test hypotheses concerning niche conservatism and geography of speciation.

Does morphology strongly correlate with current environments?

A key criterion for adaptive radiation is the presence of significant phenotype-environment correlation, which can be assessed through phylogenetic comparative analyses (Glor, 2010; Schlüter, 2000). Our phylogenetically informed linear regressions show that some morphological traits correlate with

environmental predictors but in different ways. Maximum body size is negatively correlated with temperature, with larger species generally found in cooler environments, consistent with a study indicating only fossorial snakes in Australia follow Bergmann's rule (Feldman & Meiri, 2014). However, the model-predicted differences in body size are small (0.97 mm decrease in body size per 1 °C increase) and may not have a biologically meaningful impact on the ecological niche. Feldman and Meiri (2014) suggested that in very hot areas, fossorial snakes are forced to burrow deeper into the ground, and smaller body sizes may be beneficial as this could enhance digging ability. While we were not able to explicitly test this hypothesis, we found no correlation between body size and soil bulk density or aridity index, indicating snakes of different absolute lengths are not found in areas with soil in which it is "easier" or "harder" to burrow. However, we found that body shape ratios decrease with increasing soil bulk density, suggesting that species that are "skinnier" (low MBD/SVL) occupy areas with "harder" soil to burrow. This is somewhat surprising, considering larger and more robust species of blindsnakes can generate more force to make burrows than skinnier species (Herrel et al., 2021). A possible explanation for this is that skinnier species may be using existing burrows or insect galleries instead of creating their own tunnel. If true, interspecific variation in burrowing behavior may be selected under differing environmental conditions, but testing such a hypothesis will require more in-depth microhabitat and behavior data for each species.

Fossorial movement is energetically expensive (Wu et al., 2015); therefore, we expected different snout shapes to be selected for different soil bulk densities. However, we found no correlation between dorsal snout shape and any environmental predictors. Variation in dorsal snout shape may be explained by other ecological variables we were not able to quantify, including substrate particle size, moisture content, and penetrability (Bergmann & Berry, 2021; Ehmann & Bamford, 1993). Future studies should consider cranial and axial anatomy as these may offer greater insights into variation among species (Herrel et al., 2021; Sherratt et al., 2019).

Are lineages that occupy ecologically similar habitats morphologically convergent?

Morphological convergence can be a consequence of adaptive radiation. As species diversify to exploit different niches during adaptive radiation, they may independently evolve similar adaptations in response to similar environmental challenges (Harmon et al., 2005; Roycroft et al., 2021). However, results indicate low support for morphological convergence among species that inhabit similar environments. Distance-based Ct -measures suggest that none of the arid species or humid species show any morphological convergence. Rather, body shape ratios and snout shape for all groups had negative $Ct1$ values, which suggests the phenotypic distance between species pairs is diverging from ancestral phenotype (Grossnickle et al., 2024). The frequency-based $C5$ measure indicated that humid species cross into a distinct region of snout shape, but the space defined by convergent taxa most likely included the root of the phylogeny (stem of *A. leucoproctus*) and thus should be interpreted with caution (Stayton, 2015). The evolutionary model-fitting method to test for convergence showed that the multipeak OU model was not preferred over other models. Instead, a BM model of trait evolution was preferred for body shape ratios, and the

EB model was preferred for snout shape, both suggesting a lack of convergence among lineages of interest (Grossnickle et al., 2024). One possible reason we did not find morphological convergence among species in different types of arid habitats is that the selective environment is similar in all regions, as fossorial species are buffered from extreme variation at surface conditions (Ehmann & Bamford, 1993; Ezcurra et al., 2014; Kearney et al., 2014; Nevo, 1979). Another reason is that highly specialized morphological adaptation to fossorial lifestyle may have canalized morphology and limit the number of distinct morphospace to converge on (Cyriac & Kodandaramaiah, 2018; Gans, 1969). Alternatively, there may not have been enough time or selective pressure during their time in Australia. However, the conditions of modern Australian deserts are not representative of the warm and wet conditions that precede them as recently ~2.5 Ma (Byrne et al., 2008; Pepper & Keogh, 2021). Species that occur in the arid zone today may not have experienced drastically different selective pressure compared to those in more mesic zones. Humid-environment species, on the other hand, are restricted to smaller pockets of forested areas on the east coast, which may reflect ancestral habitats. Indeed, our body shape ratios PCA show humid species tend to occupy a region of morphospace closest to that of outgroups species (Figure 2A). Species that are closely related to each other show greater similarity in morphological traits as evidenced by high phylogenetic signal, AOC tests, and sister–nonsister pairs comparisons. Overall, we observed a high degree of phenotypic conservatism, consistent with other highly specialized groups (Cyriac & Kodandaramaiah, 2018; Losos et al., 1994).

Are species predominantly allopatric or sympatric?

Nonecological speciation predicts that speciation does not arise from the divergent selection of ecological traits required for resource acquisition but rather that reproductive compatibility divergences in allopatry or parapatry (Czekanski-Moir & Rundell, 2019; Rundell & Price, 2009). We found that 9 out of 11 sister species have allopatric distributions (range overlap < 0.2), and four of these are completely isolated. In both cases where sister pairs overlap, one species has a wide-ranging distribution (*A. bituberculatus* and *A. unguirostris*), while the other's range is a small subset (*A. margaretae* and *A. yirrikalae*) of the larger range (Supplementary Figure S5).

Consistent with the range-overlap correlation tests, we found the strongest support for an allopatric-dispersal mode of speciation in blindsnakes, yet there was also competing support for a parapatric mode. Both these modes are characterized by high range size asymmetry at the point of speciation in the DREaD model (Pigot et al., 2010; Skeels & Cardillo, 2019) yet differ in whether the smaller daughter species range is close or adjacent to the parent (parapatric) or further away driven by a founder population in a new location (allopatric-dispersal). Although not investigated with the DREaD model, parapatric speciation is often associated with the divergence of the ecological niche to novel environmental conditions just outside the parent species range, for example, along an environmental cline (Loera et al., 2012; Schilthuizen et al., 2005). Given we find a model of niche conservatism for species ecological niches, we find this mode unlikely to be predominant in the clade. Instead, the speciation mode analysis, along with supporting evidence from conserved traits and niches, favors the likelihood of an allopatric-dispersal mode of

speciation. Under this model, blindsnakes may have radiated across the continent geographically, with new populations being founded in ecologically similar conditions. Blindsnakes are thought to have low dispersal capacity; however, this does not preclude the role of dispersal speciation and may even enhance its likelihood, as long- and medium-distance dispersing individuals may easily be cut off from the parent population such as in trans-oceanic dispersal (Sidharthan & Karanth, 2021; Vidal et al., 2010). Alternatively, shifts in climate or substrate may isolate a subpopulation from the parent population—which could generate a phylogenetic and geographic pattern indistinguishable from an allopatric-dispersal mode even if the true driver is a kind of vicariance. In these cases, the simulation-based approach with DREaD is unable to distinguish between modes.

Can we detect phylogenetic niche conservatism?

In general, niche overlap among both sister and nonsister pairs is much higher than geographic range overlap. These results are supported by our niche-overlap correlation test, which indicates strong evidence of phylogenetic niche conservatism. Although the observed slope and intercept from our range-overlap correlation are not different from the null expectation, we still see a pattern consistent with allopatric speciation (Fitzpatrick & Turelli, 2006).

Is there evidence for geographic radiation in allopatry?

Allopatric speciation is likely to be common on continents as it provides an opportunity for allopatric dispersal or vicariant speciation across broader geographic areas—also known as geographic radiation (Maestri et al., 2017; Simões et al., 2016). It has been hypothesized that radiations begin geographically, with populations diverging in new regions and environments as the clade spreads across a continent (Skeels & Cardillo, 2019). Ecological variation between closely related species accumulates secondarily as species begin to shift their ranges and buildup diversity in sympatry (Cotoras et al., 2018; Skeels & Cardillo, 2019; Stroud & Losos, 2020). This “geography-first” model has been shown in a similarly widespread but older Australian radiation of *Hakea* (Proteaceae) (Skeels & Cardillo, 2019) and may also explain the evolutionary history of other more recently arrived Australian arid zone radiations such as murid rodents (Roycroft et al., 2020). As blindsnakes have recently arrived on the Australian continent from Asia or New Guinea (Tiatragul et al., 2023b), this clade may currently be in the geographic radiation phase, with strong ecological differentiation in co-occurring species yet to develop.

Caveats

Ideally, to classify where on the radiation spectrum a clade should fall requires comparisons with closely related clades (Morinaga et al., 2023). Without extensive phylogenetic and morphological data on other groups of scelopophidians, we are unable to directly compare the net diversification and morphological evolution rates of Australian blindsnakes to other blindsnakes. Within the family Typhlopidae, a Sub-Saharan African blindsnake clade comprising 35 described species across two closely related genera, *Afrotyphlops* ($n = 28$) and *Rhinotyphlops* ($n = 7$) (Uetz et al., 2021), provides a potentially intriguing continental radiation comparison with the Australian blindsnakes. Future studies should

investigate if the Sub-Saharan African blindsnake clades also diversified with high morphological and ecological niche overlap.

There are also methodological limitations in our study. For example, divergent selection could be acting on niche axes other than those considered in this study, such as diet, feeding behavior, or substrate and properties of micro-habitat, all of which are poorly known for blindsnakes. A study that examined alimentary tracts of ten *Anilios* species showed pupae and larvae of ants generally made up more than 96%, except in *A. torresianus* (then referred to as *Ramphotyphlops polygrammicus*), where they found nymphs and workers of termites making up ~10% (Webb & Shine, 1993a). However, *A. torresianus* was the only species included in that study that had a tropical distribution where Australian termite biodiversity is thought to be high (Clement et al., 2021; Wijas et al., 2022). The ability of one species (*A. nigrescens*) to distinguish scent trails of ants suggests chemoreception is important in blindsnakes (Webb & Shine, 1992) and may allow specialization in certain types of prey and conspecifics like those in the Bynoe's gecko (Zozaya et al., 2019). Another limitation of our approach is that surface temperature and soil bulk density at 5cm may not accurately reflect the true microhabitats of blindsnakes and may thus be weak predictors of environmental niches (Farallo et al., 2020). For instance, the holotype of *A. longissimus* was collected on Barrow Island, Western Australia, from a section of a drilled well casing that was between 30 and 150 m deep in karst limestone (Aplin, 1998). More detailed species-specific data on diet, feeding behavior and microhabitat properties will provide a more holistic picture of blindsnake niche evolution.

Conclusion

We report the most comprehensive dataset for the continental radiation of *Anilios* blindsnakes, and our analyses reveal greater morphological variation than previously appreciated (Ehmann & Bamford, 1993; Shine & Webb, 1990). We found a degree of coupling between morphology and environment where body size negatively correlates with temperature and body shape ratios negatively correlate with soil bulk density. However, we did not find morphological convergence among species that occupy similar habitats. Consistent with the patterns observed in evolutionary radiation driven mostly by allopatric speciation, we found closely related species show some variation in morphology accompanied by a significantly high level of niche conservatism and a low level of geographic overlap. Based on these results, we suggest the continental radiation of blindsnakes in Australia aligns with the patterns associated with nonadaptive radiation (Czekanski-Moir & Rundell, 2019), which could be a common feature of recently radiated lineages that have dispersed into Australia's young arid zone.

Supplementary material

Supplementary material is available online at *Evolution*.

Data availability

Associated data and script are available at <https://zenodo.org/doi/10.5281/zenodo.10397830>

Author contributions

S.T. and S.K. conceptualized the study; S.T. collected data; S.T. analyzed the morphological data; S.T. and A.S. analyzed the niche data; S.T. prepared the figures; S.T., A.S., and S.K. wrote the manuscript.

Funding

S.K. thanks the Australian Research Council for ongoing support. S.T. was supported by the Australian Government Research Training Program Scholarship at the Australian National University.

Conflict of interest: The authors declare no conflict of interest.

Acknowledgments

We thank museum staffs from the SAM (R. Foster, S. Donnellan), Western Australian Museum (P. Doughty), Queensland Museum (A. Amey and P. Couper), Australian National Wildlife Collection (T. Haff, C. Wilson, and L. Joseph), MAGNT (G. Dally), Museums Victoria (J. Sumner, J. Melville, and R. Aguilar), FLMNH (J. Gray, C.M. Sheehy, and Z.S. Randall), and the ZMB (K. Mahlow and F. Tillack). Thanks to J. Clavel, W. Brightly, D. Grossnickle, T. Stayton, R. Shaw, E. Sherratt, O. Jimenez-Robles, C.J. Pavón Vázquez, and E. Roycroft for advice on data analyses. S.T. thanks H.C. Gerke for help with data collection, M. Pepper for advice on Australian geography, and R.J. Ellis, G. Shea, M.N. Hutchinson, S.M. Zozaya, R. Shine, D. Esquerré, and I.G. Brennan for stimulating discussions about blindsnakes.

References

- Adams, D. C., Collyer, M. L., Kaliontzopoulou, A., & Baken, E. K. (2022). *Geomorph: Software for geometric morphometric analyses*. R package version 4.0.4j.
- Aplin, K. P. (1998). Three new blindsnakes (Squamata: Typhlopidae) from northwestern Australia. *Records of the Western Australian Museum*, 19, 1–12.
- Baken, E. K., Collyer, M. L., Kaliontzopoulou, A., & Adams, D. C. (2021). Geomorph v4.0 and gmShiny: Enhanced analytics and a new graphical interface for a comprehensive morphometric experience. *Methods in Ecology and Evolution*, 12(12), 2355–2363. <https://doi.org/10.1111/2041-210x.13723>
- Bank, S., Buckley, T. R., Büscher, T. H., Bresseel, J., Constant, J., de Haan, M., Dittmar, D., Dräger, H., Kahar, R. S., Kang, A., Kneubühler, B., Langton-Myers, S. S., & Bradler, S. (2021). Reconstructing the non-adaptive radiation of an ancient lineage of ground-dwelling stick insects (Phasmatodea: Heteropterygidae). *Systematic Entomology*, 46, 487–507.
- Barley, A. J., White, J., Diesmos, A. C., & Brown, R. M. (2013). The challenge of species delimitation at the extremes: Diversification without morphological change in Philippine Sun Skinks. *Evolution*, 67(12), 3556–3572. <https://doi.org/10.1111/evo.12219>
- Barraclough, T. G., & Vogler, A. P. (2000). Detecting the geographical pattern of speciation from species-level phylogenies. *The American Naturalist*, 155(4), 419–434. <https://doi.org/10.1086/303332>
- Bergmann, P. J., & Berry, D. S. (2021). How head shape and substrate particle size affect fossorial locomotion in lizards. *The Journal of Experimental Biology*, 224(11), jeb242244. <https://doi.org/10.1242/jeb.242244>
- Bonaccorso, E., Rodríguez-Saltos, C. A., Freile, J. F., Peñafiel, N., Rosado-Llerena, L., & Oleas, N. H. (2021). Recent diversification

- in the high Andes: Unveiling the evolutionary history of the Ecuadorian hillstar, *Oreotrochilus chimborazo* (Apodiformes: Trochilidae). *Biological Journal of the Linnean Society*, 132(2), 451–470. <https://doi.org/10.1093/biolinnean/blaa200>
- Brennan, I. G., Lemmon, A. R., Lemmon, E. M., Hoskin, C. J., Donnellan, S. C., & Keogh, J. S. (2023). Populating a continent: Phylogenomics reveal the timing of Australian frog diversification. *Systematic Biology*, 73(1), 1–11. <https://doi.org/10.1093/sysbio/syad048>
- Brennan, I. G., Lemmon, A. R., Lemmon, E. M., Portik, D. M., Weijola, V., Welton, L., Donnellan, S. C., & Keogh, J. S. (2021). Phylogenomics of monitor lizards and the role of competition in dictating body size disparity. *Systematic Biology*, 70(1), 120–132. <https://doi.org/10.1093/sysbio/syaa046>
- Brennan, I. G., & Oliver, P. M. (2017). Mass turnover and recovery dynamics of a diverse Australian continental radiation. *Evolution*, 71(5), 1352–1365. <https://doi.org/10.1111/evol.13207>
- Burbrink, F. T., Grazziotin, F. G., Pyron, R. A., Cundall, D., Donnellan, S., Irish, F., Keogh, J. S., Kraus, F., Murphy, R. W., Noonan, B., Raxworthy, C. J., Ruane, S., Lemmon, A. R., Lemmon, E. M., & Zaher, H. (2020). Interrogating genomic-scale data for Squamata (lizards, snakes, and amphisbaenians) shows no support for key traditional morphological relationships. *Systematic Biology*, 69(3), 502–520. <https://doi.org/10.1093/sysbio/syz062>
- Byrne, M., Joseph, L., Yeates, D. K., Roberts, J. D., & Edwards, D. (2018). Evolutionary history. In H. Lambers (Ed.), *On the ecology of Australia's arid zone*. Springer Nature.
- Byrne, M., Steane, D. A., Joseph, L., Yeates, D. K., Jordan, G. J., Crayn, D., Aplin, K., Cantrill, D. J., Cook, L. G., Crisp, M. D., Keogh, J. S., Melville, J., Moritz, C., Porch, N., Sniderman, J. M. K., Sunnucks, P., & Weston, P. H. (2011). Decline of a biome: Evolution, contraction, fragmentation, extinction and invasion of the Australian mesic zone biota. *Journal of Biogeography*, 38(9), 1635–1656. <https://doi.org/10.1111/j.1365-2699.2011.02535.x>
- Byrne, M., Yeates, D. K., Joseph, L., Kearney, M., Bowler, J., Williams, M. A. J., Cooper, S., Donnellan, S. C., Keogh, J. S., Leys, R., Melville, J., Murphy, D. J., Porch, N., & Wyrwoll, K. -H. (2008). Birth of a biome: Insights into the assembly and maintenance of the Australian arid zone biota. *Molecular Ecology*, 17(20), 4398–4417. <https://doi.org/10.1111/j.1365-294X.2008.03899.x>
- Camaiti, M., Evans, A. R., Hipsley, C. A., Hutchinson, M. N., Meiri, S., Oliveira Anderson, R. de, Slavenko, A., & Chapple, D. G. (2023). Macroecological and biogeographical patterns of limb reduction in the world's skinks. *Journal of Biogeography*, 50, 428–440. <https://doi.org/10.1111/jbi.14547>
- Cardillo, M., Weston, P. H., Reynolds, Z. K. M., Olde, P. M., Mast, A. R., Lemmon, E. M., Lemmon, A. R., & Bromham, L. (2017). The phylogeny and biogeography of Hakea (Proteaceae) reveals the role of biome shifts in a continental plant radiation. *Evolution*, 71(8), 1928–1943. <https://doi.org/10.1111/evol.13276>
- Chaplin, K., Sumner, J., Hipsley, C. A., & Melville, J. (2020). An integrative approach using phylogenomics and high-resolution X-ray computed tomography for species delimitation in cryptic taxa. *Systematic Biology*, 69(2), 294–307. <https://doi.org/10.1093/sysbio/syz048>
- Clavel, J., Aristide, L., & Morlon, H. (2019). A penalized likelihood framework for high-dimensional phylogenetic comparative methods and an application to new-world monkeys brain evolution. *Systematic Biology*, 68(1), 93–116. <https://doi.org/10.1093/sysbio/syy045>
- Clavel, J., Escarguel, G., & Merceron, G. (2015). mvMORPH: An R package for fitting multivariate evolutionary models to morphometric data. *Methods in Ecology and Evolution*, 6(11), 1311–1319. <https://doi.org/10.1111/2041-210x.12420>
- Clavel, J., & Morlon, H. (2020). Reliable phylogenetic regressions for multivariate comparative data: illustration with the MANOVA and application to the effect of diet on mandible morphology in Phyllostomid bats. *Systematic Biology*, 69(5), 927–943. <https://doi.org/10.1093/sysbio/syaa010>
- Clement, R. A., Flores-Moreno, H., Cernusak, L. A., Cheesman, A. W., Yatsko, A. R., Allison, S. D., Eggleton, P., & Zanne, A. E. (2021). Assessing the Australian termite diversity anomaly: How habitat and rainfall affect termite assemblages. *Frontiers in Ecology and Evolution*, 9, 657444.
- Cotoras, D. D., Bi, K., Brewer, M. S., Lindberg, D. R., Prost, S., & Gillespie, R. G. (2018). Co-occurrence of ecologically similar species of Hawaiian spiders reveals critical early phase of adaptive radiation. *BMC Evolutionary Biology*, 18(1), 100. <https://doi.org/10.1186/s12862-018-1209-y>
- Couzens, A. M. C., & Prideaux, G. J. (2018). Rapid Pliocene adaptive radiation of modern kangaroos. *Science*, 362(6410), 72–75. <https://doi.org/10.1126/science.aas8788>
- Cox, C. L., & Cox, R. M. (2015). Evolutionary shifts in habitat aridity predict evaporative water loss across squamate reptiles. *Evolution*, 69(9), 2507–2516. <https://doi.org/10.1111/evol.12742>
- Crisp, M., Cook, L., & Steane, D. (2004). Radiation of the Australian flora: What can comparisons of molecular phylogenies across multiple taxa tell us about the evolution of diversity in present-day communities? *Philosophical Transactions of the Royal Society of London, Series B: Biological Sciences*, 359(1450), 1551–1571. <https://doi.org/10.1098/rstb.2004.1528>
- Cruz-Nicolás, J., Martínez-Méndez, N., Aguirre-Planter, E., Eguiarte, L. E., & Jaramillo-Correa, J. P. (2023). Niche conservatism and strong phylogenetic signals in climate, soil, and morphological variation of Neotropical firs (*Abies*, Pinaceae). *Journal of Systematics and Evolution*, 62, 368–383.
- Cruz-Nicolás, J., Villarruel-Arroyo, A., Gernandt, D. S., Fonseca, R. M., Aguirre-Planter, E., Eguiarte, L. E., & Jaramillo-Correa, J. P. (2021). Non-adaptive evolutionary processes governed the diversification of a temperate conifer lineage after its migration into the tropics. *Molecular Phylogenetics and Evolution*, 160, 107125. <https://doi.org/10.1016/j.ympev.2021.107125>
- Csilléry, K., François, O., & Blum, M. G. B. (2012). Abc: An R package for approximate Bayesian computation (ABC). *Methods in Ecology and Evolution*, 3(3), 475–479. <https://doi.org/10.1111/j.2041-210x.2011.00179.x>
- Cyriac, V. P., & Kodandaramaiah, U. (2018). Digging their own macroevolutionary grave: Fossoriality as an evolutionary dead end in snakes. *Journal of Evolutionary Biology*, 31(4), 587–598. <https://doi.org/10.1111/jeb.13248>
- Czekanski-Moir, J. E., & Rundell, R. J. (2019). The ecology of non-ecological speciation and nonadaptive radiations. *Trends in Ecology & Evolution*, 34(5), 400–415. <https://doi.org/10.1016/j.tree.2019.01.012>
- Da Silva, F. O., Fabre, A. -C., Savriama, Y., Ollonen, J., Mahlow, K., Herrel, A., Müller, J., & Di-Poi, N. (2018). The ecological origins of snakes as revealed by skull evolution. *Nature Communications*, 9(1), 376. <https://doi.org/10.1038/s41467-017-02788-3>
- Day, J. J., Martins, F. C., Tobias, J. A., & Murrell, D. J. (2020). Contrasting trajectories of morphological diversification on continents and islands in the Afrotropical white-eye radiation. *Journal of Biogeography*, 47(10), 2235–2247. <https://doi.org/10.1111/jbi.13917>
- Demos, T. C., Webala, P. W., Lutz, H. L., Kerbis Peterhans, J. C., Goodman, S. M., Cortés-Delgado, N., Bartonjo, M., & Patterson, B. D. (2020). Multilocus phylogeny of a cryptic radiation of Afro-tropical long-fingered bats (Chiroptera, Miniopteridae). *Zoologica Scripta*, 49, 1–13.
- Ehmann, H., & Bamford, M. J. (1993). Family Typhlopidae. In C. G. Glasby, G. J. B. Ross, & P. L. Beesley (Eds.), *Fauna of Australia*. Australian Government Publishing Service.
- Elith, J., Phillips, S. J., Hastie, T., Dudík, M., Chee, Y. E., & Yates, C. J. (2011). A statistical explanation of MaxEnt for ecologists. *Diversity and Distributions*, 17(1), 43–57. <https://doi.org/10.1111/j.1472-4642.2010.00725.x>
- Esparza-Estrada, C. E., Alencar, L. R. V., Terribile, L. C., Rojas-Soto, O., Yáñez-Arenas, C., & Villalobos, F. (2023). Vipers on the scene: assessing the relationship between speciation and climatic niche

- evolution in venomous snakes (Reptilia: Viperidae). *Evolutionary Biology*, 50, 264–273.
- Esquerre, D., Brennan, I. G., Donnellan, S., & Keogh, J. S. (2022). Evolutionary models demonstrate rapid and adaptive diversification of Australo-Papuan pythons. *Biology Letters*, 18(12), 20220360. <https://doi.org/10.1098/rsbl.2022.0360>
- Esquerre, D., Donnellan, S., Brennan, I. G., Lemmon, A. R., Moriarty Lemmon, E., Zaher, H., Graziotin, F. G., & Keogh, J. S. (2020). Phylogenomics, biogeography, and morphometrics reveal rapid phenotypic evolution in pythons after crossing Wallace's line. *Systematic Biology*, 69(6), 1039–1051. <https://doi.org/10.1093/sysbio/syaa024>
- Ezcurra, E., Mellink, E., & Martínez-Berdeja, A. (2014). Hot deserts. In *eLS*. John Wiley & Sons, Ltd. <https://doi.org/10.1002/9780470015902.a0003178.pub2>
- Farallo, V. R., Muñoz, M. M., Uyeda, J. C., & Miles, D. B. (2020). Scaling between macro- to microscale climatic data reveals strong phylogenetic inertia in niche evolution in plethodontid salamanders. *Evolution*, 74(5), 979–991. <https://doi.org/10.1111/evol.13959>
- Feldman, A., & Meiri, S. (2014). Australian snakes do not follow Bergmann's rule. *Evolutionary Biology*, 41(2), 327–335. <https://doi.org/10.1007/s11692-014-9271-x>
- Fick, S. E., & Hijmans, R. J. (2017). WorldClim 2: New 1-km spatial resolution climate surfaces for global land areas. *International Journal of Climatology*, 37(12), 4302–4315. <https://doi.org/10.1002/joc.5086>
- Fitzpatrick, B. M., & Turelli, M. (2006). The geography of mammalian speciation: mixed signals from phylogenies and range maps. *Evolution*, 60(3), 601–615.
- Freer, J. J., Collins, R. A., Tarling, G. A., Collins, M. A., Partridge, J. C., & Genner, M. J. (2022). Global phylogeography of hyperdiverse lanternfishes indicates sympatric speciation in the deep sea. *Global Ecology and Biogeography*, 31(11), 2353–2367. <https://doi.org/10.1111/geb.13586>
- Gans, C. (1969). Amphisbaenians-reptiles specialized for a burrowing existence. *Endeavour*, 28, 146.
- Gans, C. (1960). Studies on amphisbaenids (Amphisbaenia, Reptilia). 1, A taxonomic revision of the Trogonophinae, and a functional interpretation of the amphisbaenid adaptive pattern. *Bulletin of the American Museum of Natural History*, 119, 129–204.
- Gans, C. (1975). Tetrapod limblessness: Evolution and functional corollaries. *American Zoologist*, 15(2), 455–467. <https://doi.org/10.1093/icb/15.2.455>
- Gillespie, R. G., Bennett, G. M., De Meester, L., Feder, J. L., Fleischer, R. C., Harmon, L. J., Hendry, A. P., Knape, M. L., Mallet, J., Martin, C., Parent, C. E., Patton, A. H., Pfennig, K. S., Rubinoff, D., Schluter, D., Seehausen, O., Shaw, K. L., Stacy, E., Stervander, M., ... Wogan, G. O. (2020). Comparing adaptive radiations across space, time, and taxa. *Journal of Heredity*, 111, 1–20.
- Gittenberger, E. (1991). What about non-adaptive radiation? *Biological Journal of the Linnean Society*, 43(4), 263–272. <https://doi.org/10.1111/j.1095-8312.1991.tb00598.x>
- Glor, R. E. (2010). Phylogenetic insights on adaptive radiation. *Annual Review of Ecology, Evolution, and Systematics*, 41(1), 251–270. <https://doi.org/10.1146/annurev.ecolsys.39.110707.173447>
- Grant, P. R., & Grant, B. R. (2014). *40 years of evolution: Darwin's finches on Daphne Major Island*. Princeton University Press.
- Gray, J. A., Sherratt, E., Hutchinson, M. N., & Jones, M. E. H. (2019). Evolution of cranial shape in a continental-scale evolutionary radiation of Australian lizards. *Evolution*, 73(11), 2216–2229. <https://doi.org/10.1111/evol.13851>
- Greenwell, B. M., & Boehmke, B. C. (2020). Variable importance plots—An introduction to the vip package. *The R Journal*, 12, 343–366.
- Grossnickle, D. M., Brightly, W. H., Weaver, L. N., Stanchak, K. E., Roston, R. A., Pevsner, S. K., Stayton, C. T., Polly, P. D., & Law, C. J. (2024). Challenges and advances in measuring phenotypic convergence. *Evolution*, 78(8), 1355–1371. <https://doi.org/10.1093/evolut/qpae081>
- Grundler, M. C., & Rabosky, D. L. (2014). Trophic divergence despite morphological convergence in a continental radiation of snakes. *Proceedings Biological Sciences*, 281(1787), 20140413. <https://doi.org/10.1098/rspb.2014.0413>
- Gunz, P., & Mitteroecker, P. (2013). Semilandmarks: A method for quantifying curves and surfaces. *Hystrix, the Italian Journal of Mammalogy*, 24, 103–109.
- Harmon, L. J., Kolbe, J. J., Cheverud, J. M., & Losos, J. B. (2005). Convergence and the multidimensional niche. *Evolution*, 59(2), 409–421.
- Hausdorf, B., & Xu, J. (2023). Speciation of rock-dwelling snail species: Disjunct ranges and mosaic patterns reveal the importance of long-distance dispersal in *Chilostoma* (Cingulifera) in the European Southern Alps. *Molecular Phylogenetics and Evolution*, 184, 107788. <https://doi.org/10.1016/j.ympev.2023.107788>
- Herrando-Moraira, S., Roquet, C., Calleja, J. -A., Chen, Y. -S., Fujikawa, K., Galbany-Casals, M., Garcia-Jacas, N., Liu, J. -Q., López-Alvarado, J., López-Pujol, J., Mandel, J. R., Mehregan, I., Sáez, L., Sennikov, A. N., Susanna, A., Vilatersana, R., & Xu, L. -S. (2023). Impact of the climatic changes in the Pliocene-Pleistocene transition on Irano-Turanian species. The radiation of genus *Jurinea* (Compositae). *Molecular Phylogenetics and Evolution*, 189, 107928.
- Herrel, A., Lowie, A., Miralles, A., Gaucher, P., Kley, N. J., Measey, J., & Tolley, K. A. (2021). Burrowing in blindsnakes: A preliminary analysis of burrowing forces and consequences for the evolution of morphology. *Anatomical Record (Hoboken, N. J.: 2007)*, 304(10), 2292–2302. <https://doi.org/10.1002/ar.24686>
- Heterick, B. E., Castalanelli, M., & Shattuck, S. O. (2017). Revision of the ant genus *Melophorus* (Hymenoptera, Formicidae). *ZooKeys*, 700, 1–420. <https://doi.org/10.3897/zookeys.700.11784>
- Hijmans, R. J. (2023). *Raster: Geographic data analysis and modeling*. R package version 3.6-26. <https://CRAN.R-project.org/package=raster>
- Ho, L. S. T., & Ane, C. (2014). A linear-time algorithm for Gaussian and non-Gaussian trait evolution models. *Systematic Biology*, 63, 397–408.
- Holland, B. S., & Hadfield, M. G. (2004). Origin and diversification of the endemic Hawaiian tree snails (Achatinellidae: Achatinellinae) based on molecular evidence. *Molecular Phylogenetics and Evolution*, 32(2), 588–600. <https://doi.org/10.1016/j.ympev.2004.01.003>
- Kearney, M. R., Shamakhy, A., Tingley, R., Karoly, D. J., Hoffmann, A. A., Briggs, P. R., & Porter, W. P. (2014). Microclimate modelling at macro scales: A test of a general microclimate model integrated with gridded continental-scale soil and weather data. *Methods in Ecology and Evolution*, 5(3), 273–286. <https://doi.org/10.1111/2041-210x.12148>
- Klingenberg, C. P. (2016). Size, shape, and form: Concepts of allometry in geometric morphometrics. *Development Genes and Evolution*, 226(3), 113–137. <https://doi.org/10.1007/s00427-016-0539-2>
- Koch, E. L., Neiber, M. T., Walther, F., & Hausdorf, B. (2020). Patterns and processes in a non-adaptive radiation: *Alopia* (Gastropoda, Clausiliidae) in the Bucegi Mountains. *Zoologica Scripta*, 49(3), 280–294. <https://doi.org/10.1111/zsc.12406>
- Kornfield, I., & Smith, P. F. (2000). African cichlid fishes: Model systems for evolutionary biology. *Annual Review of Ecology and Systematics*, 31(1), 163–196. <https://doi.org/10.1146/annurev.ecolsys.31.1.163>
- Kozak, K. H., Weisrock, D. W., & Larson, A. (2006). Rapid lineage accumulation in a non-adaptive radiation: Phylogenetic analysis of diversification rates in eastern North American woodland salamanders (Plethodontidae: *Plethodon*). *Proceedings Biological Sciences*, 273(1586), 539–546. <https://doi.org/10.1098/rspb.2005.3326>
- Lee, M. S. Y., Sanders, K. L., King, B., & Palci, A. (2016). Diversification rates and phenotypic evolution in venomous snakes (Elapidae). *Royal Society Open Science*, 3(1), 150277. <https://doi.org/10.1098/rsos.150277>
- Loera, I., Sosa, V., & Ickert-Bond, S. M. (2012). Diversification in North American arid lands: Niche conservatism, divergence and

- expansion of habitat explain speciation in the genus *Ephedra*. *Molecular Phylogenetics and Evolution*, 65(2), 437–450. <https://doi.org/10.1016/j.ympev.2012.06.025>
- Losos, J. B. (2009). *Lizards in an evolutionary tree: Ecology and adaptive radiation of anoles*. University of California Press.
- Losos, J. B., Irschick, D. J., & Schoener, T. W. (1994). Adaptation and constraint in the evolution of specialization of Bahamian *Anolis* lizards. *Evolution*, 48(6), 1786–1798. <https://doi.org/10.1111/j.1558-5646.1994.tb02214.x>
- Mabbutt, J. A. (1988). Australian desert landscapes. *GeoJournal*, 16(4), 355–369.
- Maestri, R., Monteiro, L. R., Fornel, R., Upham, N. S., Patterson, B. D., & de Freitas, T. R. O. (2017). The ecology of a continental evolutionary radiation: Is the radiation of sigmodontine rodents adaptive? *Evolution*, 71, 610–632.
- Marin, J., Donnellan, S. C., Hedges, S. B., Doughty, P., Hutchinson, M. N., Cruaud, C., & Vidal, N. (2013a). Tracing the history and biogeography of the Australian blindsnake radiation. *Journal of Biogeography*, 40, 928–937.
- Marin, J., Donnellan, S. C., Hedges, S. B., Puillandre, N., Aplin, K. P., Doughty, P., Hutchinson, M. N., Couloux, A., & Vidal, N. (2013b). Hidden species diversity of Australian burrowing snakes (*Ramphotyphlops*). *Biological Journal of the Linnean Society*, 110(2), 427–441. <https://doi.org/10.1111/bij.12132>
- Marki, P. Z., Jönsson, K. A., Irestedt, M., Nguyen, J. M. T., Rahbek, C., & Fjeldså, J. (2017). Supermatrix phylogeny and biogeography of the Australasian Meliphagidae radiation (Aves: Passeriformes). *Molecular Phylogenetics and Evolution*, 107, 516–529. <https://doi.org/10.1016/j.ympev.2016.12.021>
- Minh, B. Q., Schmidt, H. A., Chernomor, O., Schrempf, D., Woodhams, M. D., von Haeseler, A., & Lanfear, R. (2020). IQ-TREE 2: New models and efficient methods for phylogenetic inference in the genomic era. *Molecular Biology and Evolution*, 37(5), 1530–1534. <https://doi.org/10.1093/molbev/msaa015>
- Miralles, A., Marin, J., Markus, D., Herrel, A., Hedges, S. B., & Vidal, N. (2018). Molecular evidence for the paraphyly of Scolecophidia and its evolutionary implications. *Journal of Evolutionary Biology*, 31(12), 1782–1793. <https://doi.org/10.1111/jeb.13373>
- Morinaga, G., Wiens, J. J., & Moen, D. S. (2023). The radiation continuum and the evolution of frog diversity. *Nature Communications*, 14(1), 7100. <https://doi.org/10.1038/s41467-023-42745-x>
- Moritz, C., Fujita, M. K., Rosauer, D., Agudo, R., Bourke, G., Doughty, P., Palmer, R., Pepper, M., Potter, S., Pratt, R., Scott, M., Tonione, M., & Donnellan, S. (2016). Multilocus phylogeography reveals nested endemism in a gecko across the monsoonal tropics of Australia. *Molecular Ecology*, 25(6), 1354–1366. <https://doi.org/10.1111/mec.13511>
- Mosimann, J. E. (1970). Size allometry: Size and shape variables with characterizations of the lognormal and generalized gamma distributions. *Journal of the American Statistical Association*, 65(330), 930–945. <https://doi.org/10.2307/2284599>
- Nevo, E. (1979). Adaptive convergence and divergence of subterranean mammals. *Annual Review of Ecology and Systematics*, 10(1), 269–308. <https://doi.org/10.1146/annurev.es.10.110179.001413>
- Norris, J., Tingley, R., Meiri, S., & Chapple, D. G. (2021). Environmental correlates of morphological diversity in Australian geckos. *Global Ecology and Biogeography*, 30(5), 1086–1100. <https://doi.org/10.1111/geb.13284>
- Olivares, I., Tusso, S., José Sanín, M., Harpe, M. de La, Loiseau, O., Rolland, J., Salamin, N., Kessler, M., Shimizu, K. K., & Paris, M. (2024). Hyper-cryptic radiation of a tropical montane plant lineage. *Molecular Phylogenetics and Evolution*, 190, 107954.
- Oliver, P. M., Adams, M., Lee, M. S. Y., Hutchinson, M. N., & Doughty, P. (2009). Cryptic diversity in vertebrates: Molecular data double estimates of species diversity in a radiation of Australian lizards (*Diplodactylus*, Gekkota). *Proceedings of the Royal Society B: Biological Sciences*, 276, 2001–2007.
- Oliver, P. M., & Hugall, A. F. (2017). Phylogenetic evidence for mid-Cenozoic turnover of a diverse continental biota. *Nature Ecology & Evolution*, 1(12), 1896–1902. <https://doi.org/10.1038/s41559-017-0355-8>
- Osorio-Olvera, L., Lira-Noriega, A., Soberón, J., Peterson, A. T., Falconi, M., Contreras-Díaz, R. G., Martínez-Meyer, E., Barve, V., & Barve, N. (2020). Ntbox: An r package with graphical user interface for modelling and evaluating multidimensional ecological niches. *Methods in Ecology and Evolution*, 11, 1199–1206.
- Owen, C. L., Marshall, D. C., Hill, K. B. R., & Simon, C. (2017). How the aridification of Australia structured the biogeography and influenced the diversification of a large lineage of Australian cicadas. *Systematic Biology*, 66(4), 569–589. <https://doi.org/10.1093/sysbio/syw078>
- Pavón-Vázquez, C. J., Esquerré, D., & Keogh, J. S. (2022). Ontogenetic drivers of morphological evolution in monitor lizards and allies (Squamata: Paleoanguiomorpha), a clade with extreme body size disparity. *BMC Ecology and Evolution*, 22(1), 15. <https://doi.org/10.1186/s12862-022-01970-6>
- Pepper, M., & Keogh, J. S. (2021). Life in the “dead heart” of Australia: The geohistory of the Australian deserts and its impact on genetic diversity of arid zone lizards. *Journal of Biogeography*, 48(4), 716–746. <https://doi.org/10.1111/jbi.14063>
- Pie, M. R., Campos, L. L. F., Meyer, A. L. S., & Duran, A. (2017). The evolution of climatic niches in squamate reptiles. *Proceedings Biological Sciences*, 284(1858), 20170268. <https://doi.org/10.1098/rspb.2017.0268>
- Pigot, A. L., Phillimore, A. B., Owens, I. P. F., & Orme, C. D. L. (2010). The shape and temporal dynamics of phylogenetic trees arising from geographic speciation. *Systematic Biology*, 59(6), 660–673. <https://doi.org/10.1093/sysbio/syq058>
- Prates, I., Hutchinson, M. N., Singhal, S., Moritz, C., & Rabosky, D. L. (2023). Notes from the taxonomic disaster zone: Evolutionary drivers of intractable species boundaries in an Australian lizard clade (Scincidae: *Ctenotus*). *Molecular Ecology*, 1–25. <https://doi.org/10.1111/mec.17074>
- Rabosky, D. L., Donnellan, S. C., Talaba, A. L., & Lovette, I. J. (2007). Exceptional among-lineage variation in diversification rates during the radiation of Australia’s most diverse vertebrate clade. *Proceedings Biological Sciences*, 274(1628), 2915–2923. <https://doi.org/10.1098/rspb.2007.0924>
- Ramírez-Reyes, T., Velasco, J. A., Flores-Villela, O., & Piñero, D. (2022). Decoupling in diversification and body size rates during the radiation of *Phyllodactylus*: Evidence suggests minor role of ecology in shaping phenotypes. *Evolutionary Biology*, 49(3), 373–387. <https://doi.org/10.1007/s11692-022-09575-z>
- Reaney, A. M., Saldarriaga-Córdoba, M., & Pincheira-Donoso, D. (2018). Macroevolutionary diversification with limited niche disparity in a species-rich lineage of cold-climate lizards. *BMC Evolutionary Biology*, 18(1), 16. <https://doi.org/10.1186/s12862-018-1133-1>
- Revell, L. J. (2012). Phytools: An R package for phylogenetic comparative biology (and other things). *Methods in Ecology and Evolution*, 3(2), 217–223. <https://doi.org/10.1111/j.2041-210x.2011.00169.x>
- Rohlf, F. (2015). The tps series of software. *Hystrix, the Italian Journal of Mammalogy*, 26, 9–12.
- Roycroft, E. J., Nations, J. A., & Rowe, K. C. (2020). Environment predicts repeated body size shifts in a recent radiation of Australian mammals. *Evolution*, 74(3), 671–680. <https://doi.org/10.1111/evol.13859>
- Roycroft, E., Achmadi, A., Callahan, C. M., Esselstyn, J. A., Good, J. M., Moussalli, A., & Rowe, K. C. (2021). Molecular evolution of ecological specialisation: Genomic insights from the diversification of murine rodents. *Genome Biology and Evolution*, 13(7), evab103. <https://doi.org/10.1093/gbe/evab103>
- Roycroft, E., Fabre, P.-H., MacDonald, A. J., Moritz, C., Moussalli, A., & Rowe, K. C. (2022). New Guinea uplift opens ecological opportunity across a continent. *Current Biology: CB*, 32(19), 4215–4224.e3. <https://doi.org/10.1016/j.cub.2022.08.021>
- Rundell, R. J., & Price, T. D. (2009). Adaptive radiation, nonadaptive radiation, ecological speciation and nonecological speciation.

- Trends in Ecology & Evolution*, 24(7), 394–399. <https://doi.org/10.1016/j.tree.2009.02.007>
- Sanders, K. L., Lee, M. S. Y., Leys, R., Foster, R., & Keogh, J. S. (2008). Molecular phylogeny and divergence dates for Australasian elapids and sea snakes (Hydrophiinae): Evidence from seven genes for rapid evolutionary radiations. *Journal of Evolutionary Biology*, 21(3), 682–695. <https://doi.org/10.1111/j.1420-9101.2008.01525.x>
- Schlithuizen, M., Cabanban, A. S., & Haase, M. (2005). Possible speciation with gene flow in tropical cave snails. *Journal of Zoological Systematics and Evolutionary Research*, 43(2), 133–138. <https://doi.org/10.1111/j.1439-0469.2004.00289.x>
- Schlüter, D. (2000). *The ecology of adaptive radiation*. Oxford University Press.
- Schneider, C., & Moritz, C. (1999). Rainforest refugia and Australia's wet tropics. *Proceedings of the Royal Society of London. Series B: Biological Sciences*, 266(1415), 191–196. <https://doi.org/10.1098/rspb.1999.0621>
- Sherratt, E., Sanders, K. L., Watson, A., Hutchinson, M. N., Lee, M. S. Y., & Palci, A. (2019). Heterochronic shifts mediate ecomorphological convergence in skull shape of microcephalic sea snakes. *Integrative and Comparative Biology*, 59(3), 616–624. <https://doi.org/10.1093/icb/icz033>
- Shine, R., & Webb, J. K. (1990). Natural history of Australian Typhlopidae snakes. *Journal of Herpetology*, 24(4), 357–363. <https://doi.org/10.2307/1565050>
- Sidharthan, C., & Karanth, K. P. (2021). India's biogeographic history through the eyes of blindsnares- filling the gaps in the global typhlopoid phylogeny. *Molecular Phylogenetics and Evolution*, 157, 107064. <https://doi.org/10.1016/j.ympev.2020.107064>
- Simões, M., Breitkreuz, L., Alvarado, M., Baca, S., Cooper, J. C., Heins, L., Herzog, K., & Lieberman, B. S. (2016). The evolving theory of evolutionary radiations. *Trends in Ecology & Evolution*, 31(1), 27–34. <https://doi.org/10.1016/j.tree.2015.10.007>
- Simpson, G. G. (1953). *The major features of evolution*. Columbia University Press.
- Singhal, S., Hoskin, C. J., Couper, P., Potter, S., & Moritz, C. (2018). A framework for resolving cryptic species: A case study from the lizards of the Australian wet tropics. *Systematic Biology*, 67(6), 1061–1075. <https://doi.org/10.1093/sysbio/syy026>
- Skeels, A., Boschman, L. M., McFadden, I. R., Joyce, E. M., Hagen, O., Jiménez Robles, O., Bach, W., Boussange, V., Keggins, T., Jetz, W., & Pellissier, L. (2023). Paleoenvironments shaped the exchange of terrestrial vertebrates across Wallace's Line. *Science*, 381(6653), 86–92. <https://doi.org/10.1126/science.adf7122>
- Skeels, A., & Cardillo, M. (2019). Reconstructing the geography of speciation from contemporary biodiversity data. *The American Naturalist*, 193(2), 240–255. <https://doi.org/10.1086/701125>
- Stayton, C. T. (2015). The definition, recognition, and interpretation of convergent evolution, and two new measures for quantifying and assessing the significance of convergence. *Evolution*, 69(8), 2140–2153. <https://doi.org/10.1111/evol.12729>
- Stroud, J. T., & Losos, J. B. (2020). Bridging the process-pattern divide to understand the origins and early stages of adaptive radiation: A review of approaches with insights from studies of *Anolis* lizards. *The Journal of Heredity*, 111(1), 33–42. <https://doi.org/10.1093/jhered/esz055>
- Stroud, J. T., & Losos, J. B. (2016). Ecological opportunity and adaptive radiation. *Annual Review of Ecology, Evolution, and Systematics*, 47(1), 507–532. <https://doi.org/10.1146/annurev-ecolsys-121415-032254>
- Tiatragul, S., Brennan, I. G., Broady, E. S., & Keogh, J. S. (2023a). Australia's hidden radiation: Phylogenomics analysis reveals rapid Miocene radiation of blindsnares. *Molecular Phylogenetics and Evolution*, 185, 107812. <https://doi.org/10.1016/j.ympev.2023.107812>
- Tiatragul, S., Skeels, A., & Keogh, J. S. (2023b). Paleoenvironmental models for Australia and the impact of aridification on blindsnares diversification. *Journal of Biogeography*, 50(11), 1899–1913. <https://doi.org/10.1111/jbi.14700>
- Uetz, P., Koo, M. S., Aguilar, R., Brings, E., Catenazzi, A., Chang, A. T., & Wake, D. B. (2021). A quarter century of reptile and amphibian databases. *Herpetological Review*, 52, 246–255.
- Uyeda, J. C., Caetano, D. S., & Pennell, M. W. (2015). Comparative analysis of principal components can be misleading. *Systematic Biology*, 64(4), 677–689. <https://doi.org/10.1093/sysbio/syv019>
- Vidal, N., Marin, J., Morini, M., Donnellan, S., Branch, W. R., Thomas, R., Vences, M., Wynn, A., Cruaud, C., & Hedges, S. B. (2010). Blindsnares evolutionary tree reveals long history on Gondwana. *Biology Letters*, 6(4), 558–561. <https://doi.org/10.1098/rsbl.2010.0220>
- Waite, E. R. (1894). Notes on Australian Typhlopidae. *Proceedings of the Linnean Society of New South Wales*, 9, 9–14. <https://doi.org/10.5962/bhl.part.18087>
- Wake, D. B. (2006). Problems with species: Patterns and processes of species formation in salamanders. *Annals of the Missouri Botanical Garden*, 93(1), 8–23. [https://doi.org/10.3417/0026-6493\(2006\)93\[8:pwpap\]2.0.co;2](https://doi.org/10.3417/0026-6493(2006)93[8:pwpap]2.0.co;2)
- Warren, D. L., Matzke, N. J., Cardillo, M., Baumgartner, J. B., Beaumont, L. J., Turelli, M., Glor, R. E., Huron, N. A., Simões, M., Iglesias, T. L., Piquet, J. C., & Dinnage, R. (2021). ENMTTools 1.0: An R package for comparative ecological biogeography. *Ecography*, 44(4), 504–511. <https://doi.org/10.1111/ecog.05485>
- Webb, J. K., & Shine, R. (1993a). Dietary habits of Australian blindsnares (Typhlopidae). *Copeia*, 1993(3), 762–770. <https://doi.org/10.2307/1447239>
- Webb, J. K., & Shine, R. (1993b). Prey-size selection, gape limitation and predator vulnerability in Australian blindsnares (Typhlopidae). *Animal Behaviour*, 45(6), 1117–1126. <https://doi.org/10.1006/anbe.1993.1136>
- Webb, J. K., & Shine, R. (1992). To find an ant: Trail-following in Australian blindsnares (Typhlopidae). *Animal Behaviour*, 43, 941–948.
- Wellenreuther, M., & Sánchez-Guillén, R. A. (2016). Nonadaptive radiation in damselflies. *Evolutionary Applications*, 9(1), 103–118. <https://doi.org/10.1111/eva.12269>
- Werner, F. (1901). Ueber Reptilien und Batrachier aus Ecuador und Neu-Guinea. *Verhandlungen der Kaiserlich-Königlichen Zoologisch-Botanischen Gesellschaft in Wien*, 51, 593–614.
- Wiens, J. J., Kozak, K. H., & Silva, N. (2013). Diversity and niche evolution along aridity gradients in North American lizards (Phrynosomatidae). *Evolution*, 67(6), 1715–1728. <https://doi.org/10.1111/evo.12053>
- Wijas, B. J., Lim, S., & Cornwell, W. K. (2022). Continental-scale shifts in termite diversity and nesting and feeding strategies. *Ecography*, 2022(1), e05902. <https://doi.org/10.1111/ecog.05902>
- Wilke, T., Benke, M., Brändle, M., Albrecht, C., & Bichain, J. -M. (2010). The neglected side of the coin: Non-adaptive radiations in spring snails (*Bythinella* spp.). In M. Glaubrecht (Ed.), *Evolution in action: Case studies in adaptive radiation, speciation and the origin of biodiversity* (pp. 551–578). Springer.
- Wu, N. C., Alton, L. A., Clemente, C. J., Kearney, M. R., & White, C. R. (2015). Morphology and burrowing energetics of semi-fossorial skinks (*Liopholis* spp.). *The Journal of Experimental Biology*, 218(Pt 15), 2416–2426. <https://doi.org/10.1242/jeb.113803>
- Xu, M., & Shaw, K. L. (2020). Spatial mixing between calling males of two closely related, sympatric crickets suggests beneficial heterospecific interactions in a nonadaptive radiation. *The Journal of Heredity*, 111(1), 84–91. <https://doi.org/10.1093/jhered/esz062>
- Yang, Z. (2007). PAML 4: Phylogenetic analysis by maximum likelihood. *Molecular Biology and Evolution*, 24(8), 1586–1591. <https://doi.org/10.1093/molbev/msm088>
- Zhang, C., Rabiee, M., Sayyari, E., & Mirarab, S. (2018). ASTRAL-III: Polynomial time species tree reconstruction from partially resolved gene trees. *BMC Bioinformatics*, 19(S6), 153.
- Zomer, R. J., Xu, J., & Trabucco, A. (2022). Version 3 of the global aridity index and potential evapotranspiration database. *Scientific Data*, 9(1), 409. <https://doi.org/10.1038/s41597-022-01493-1>
- Zozaya, S. M., Higgle, M., Moritz, C., & Hoskin, C. J. (2019). Are pheromones key to unlocking cryptic lizard diversity? *The American Naturalist*, 194(2), 168–182. <https://doi.org/10.1086/704059>